NOTICE

The quality of this microform is heavily dependent upon the quality of the original thesis submitted for microfilming. Every effort has been made to ensure the highest quality of reproduction possible.

If pages are missing, contact the university which granted the degree.

Some pages may have indistinct print especially if the original pages were typed with a poor typewriter ribbon or if the university sent us an inferior photocopy.

Previously copyrighted materials (journal articles, published tests, etc.) are not filmed.

Reproduction in full or in part of this microform is governed by the Canadian Copyright Act, R.S.C. 1970, c. C-30.

AVIS

La qualité de cette microforme dépend grandement de la qualité de la thèse soumise au microfilmage. Nous avons tout fait pour assurer une qualité supérieure de reproduction.

S'il manque des pages, veuillez communiquer avec l'université qui a conféré le grade.

La qualité d'impression de certaines pages peut laisser à désirer, surtout si les pages originales ont été dactylographiées à l'aide d'un ruban usé ou si l'université nous a fait parvenir une photocopie de qualité inférieure.

Les documents qui font déjà l'objet d'un droit d'auteur (articles de revue, tests publiés, etc.) ne sont pas microfilmés.

La reproduction, même partielle, de cette microforme est soumise à la Loi canadienne sur le droit d'auteur, SRC 1970, c. C-30.

Canada

THE EXTRACTION OF VEGETABLE OILS FROM POTATO CHIPS USING SUPERCRITICAL CARBON DIOXIDE

by

Alfred John O'Neill

A thesis

presented to the University of Ottawa

in fulfillment of the

thesis requirement for the degree of

Master of Applied Science

in

Chemical Engineering

Department of Chemical Engineering

University of Ottawa

Ottawa, Ontario, 1987

ISBN 0-315-46833-5

UNIVERSITÉ D'OTTAWA
UNIVERSITY OF OTTAWA

ABSTRACT

The extraction of vegetable oil from potato chips using supercritical carbon dioxide is examined from a practical viewpoint. A factorial design is used to locate the variables of primary influence on oil solubility. Emphasis is placed on locating the optimum operating regions. Both batch and flow processes are used to study the effect of pressure and flowrate on oil removal and recovery. Data are fitted to the Chrastil equation to facilitate solubility prediction over a range of pressures.

The survivability and marketability of the chips are appraised by a qualitative analysis of the final product. A chromatographic analysis of natural and extracted vegetable oil is performed to determine the degree of fractionation, if any, resulting from the process.

ACKNOWLEDGMENTS

The author would like to express his sincere thanks to Doctor B.C.-Y. Lu, Professor of Chemical Engineering at the University of Ottawa, for his wisdom and guidance in overseeing the project from inception to completion. The assistance of the technical staff of the Chemical Engineering Department of the University of Ottawa was also greatly appreciated during the construction of the apparatus. Thanks go out to Mr. J. Gasperetti, Mr. D. Lefebvre, and Mr. A. Bonaldo.

NOMENCLATURE

A_i: Probability of Selecting Choice A

a: Chrastil Solubility Constant

b: Chrastil Solubility Constant

c: Concentration of Solute (g/ml)

CP_i: Critical Endpoint of Vapour Pressure Curve for Component i

d: Fluid Density (g/ml)

K: Chrastil Solubility Constant

m: Mass of Solute (g)

N: Number of Runs

P_c: Critical Pressure

P^{sat}: Saturation Pressure

T_c: Critical Temperature

$\overline{V}_i$: Partial Molar Volume of Component i

W: Amalgamated Solubility Constant

x_i: Mole Fraction i

X1: Temperature Coded Variable

X2: Pressure Coded Variable

X3: Purge Rate Coded Variable

X4: Retention Time Coded Variable

$\hat{Y}$: Fitted Response (Oil Removed, g)

TABLE OF CONTENTS

APPENDICES

LIST OF FIGURES

LIST OF TABLES

Chapter I

INTRODUCTION

In recent years the use of supercritical fluids as solvents has found widening applications in industry. The process, known as supercritical fluid extraction (SFE), is based on the fact that the solubility of many components in supercritical fluids may be from five to twelve orders of magnitude higher than the ideal solubility expected from the vapour pressure of the solute. While the properties of supercritical fluids, specifically the high temperature and pressure required for most gases to attain the supercritical state, may not at first seem conducive to their use as industrial solvents, their high solvent power and unusual physical properties make them ideally suitable for a number of commercial applications.

It is the dual nature of the supercritical fluid (SCF), which exhibits both gas and liquid behavior, that results in its usefulness as an extraction medium. Common supercritical fluids have a density of from thirty to eighty percent that of normal fluids. The physical properties of supercritical fluids are summarized in Table 1 and compared to those of a liquid and gas. The SCF is carbon dioxide near its critical point.

The advantages of supercritical fluids may be clearly

seen from this table. There is less resistance to mass transfer than in a liquid, while viscosities are generally an order of magnitude lower. Solubilities are much higher than in a gas, and precipitation of dissolved material is accomplished by a decrease in the solvent density, which may be controlled by manipulation of temperature or pressure. The solute is always a heavy component.

The major disadvantage of SFE is the high capital cost of equipment. Most SFE processes are energy-intensive as a result of the high temperature and pressure required, and therefore expensive. In addition the scarcity of fundamental engineering data, specifically solubility data and phase diagrams for complex systems, has hindered progress. Direct experimental determination of solubility data at high pressure requires considerable time and expense, and the accuracy of most methods of correlation and prediction of solubility is questionable in the supercritical region.

While the problem of available data in the literature continues to improve, the high capital cost of equipment remains a drawback. As a result research emphasis has been on separations which are difficult to do any other way, and result in products which are expensive enough to bear the burden of the additional processing. While this eliminates commodity chemicals, it does leave open the field of higher purity (and necessarily higher priced) products such as drugs and speciality polymers, as well as the more expensive food

Table 1: PROPERTIES OF A SUPERCRITICAL FLUID

FLUID	DENSITY g/ml	VISCOSITY cp	DIFFUSION COEFFICIENT cm^2/g
Supercritical fluid	0.7	0.01	0.01
Gas	0.001	0.001	0.1
Liquid	1	0.1	0.00001

products such as coffee and snack foods.

The choice of supercritical solvent has perhaps the greatest influence on the operating costs of the system. Carbon dioxide is the most common solvent in use today, in both industry and the laboratory. The choice of carbon dioxide is made on the basis of its attractive physical properties: it is non-toxic, nonflammable, noncorrosive to steel and most plastics, has a low critical temperature (31.2° C), and more importantly a relatively low critical pressure (7.38 MPa, or 1069 psi). Additionally, it is cheap, readily available, and is the solvent for which the largest body of data has been collected.

Background and Theory

The fact that compressed gases can dissolve solids was first demonstrated by Hanny and Hogarth in 1879 (1). By the mid 1950's several researchers suggested supercritical fluid extraction as an alternative to conventional separation techniques such as distillation and liquid extraction. Further development in the early seventies led to supercritical carbon dioxide being introduced for use in food preparation. As a result, for the first time natural products such as coffee, tobacco, spices, hops, and cocoa could be extracted without the need for organic solvents.

The Arthur D. Little process, developed at M.I.T., used carbon dioxide to demonstrate the versatility of supercritical solvents (2). The process could operate in both batch and continuous fashion, and was capable of multiple-step separations of various adsorbate components, accomplished by manipulating the temperature. This was possible because a supercritical fluid may be a nonsolvent for one component at a particular temperature while remaining a solvent for all other components.

Today, many proposals for SFE are being submitted by the petrochemical, pharmaceutical, and food industries. This is a result of the more stringent standards for drug purity, as set by the American Food and Drug Administration and Health and Welfare Canada, as well as attempts to economically process lower grade petrochemical feedstocks, for example naturally polluted fuels, and a shift in process emphasis due to rapidly increasing energy costs.

Extraction with supercritical fluids has many advantages over both distillation and conventional solvent extraction. Many fluid extractions may be performed at room temperature, avoiding the danger of thermally decomposing unstable substances which often occurs during distillation. Liquid extraction can require a crystallization procedure for separation purposes which may leave residual solvent in the extract. In the case of SFE however, extract separation

involves decreasing the density of the solvent to the gaseous phase so that very little if any of the solvent is left in the product. Moreover, both the selectivity and solvent power can be carefully controlled through temperature, pressure, and choice of solvent. Controlling the extraction with temperature results in significant energy savings over such energy-intensive processes as distillation.

The supercritical region of any pure substance is defined by both its critical temperature and its critical pressure. On a phase diagram, it may be represented as the region beyond the termination of the vaporization curve (see Figure 1). The critical pressure P_c and critical temperature T_c represent the highest temperature and pressure at which a pure substance can exist in vapour-liquid equilibrium. A phase is considered to be a vapour if it can be condensed by a reduction of temperature at constant pressure, and a liquid if it can be vaporized by a reduction in pressure at constant temperature. As the fluid region fits neither of these definitions, a substance existing in this region is said to be in the supercritical phase.

The solubility of a solute in any solvent varies directly with the density of the solvent, as well as more subtle factors such as the di-electric constant. For a

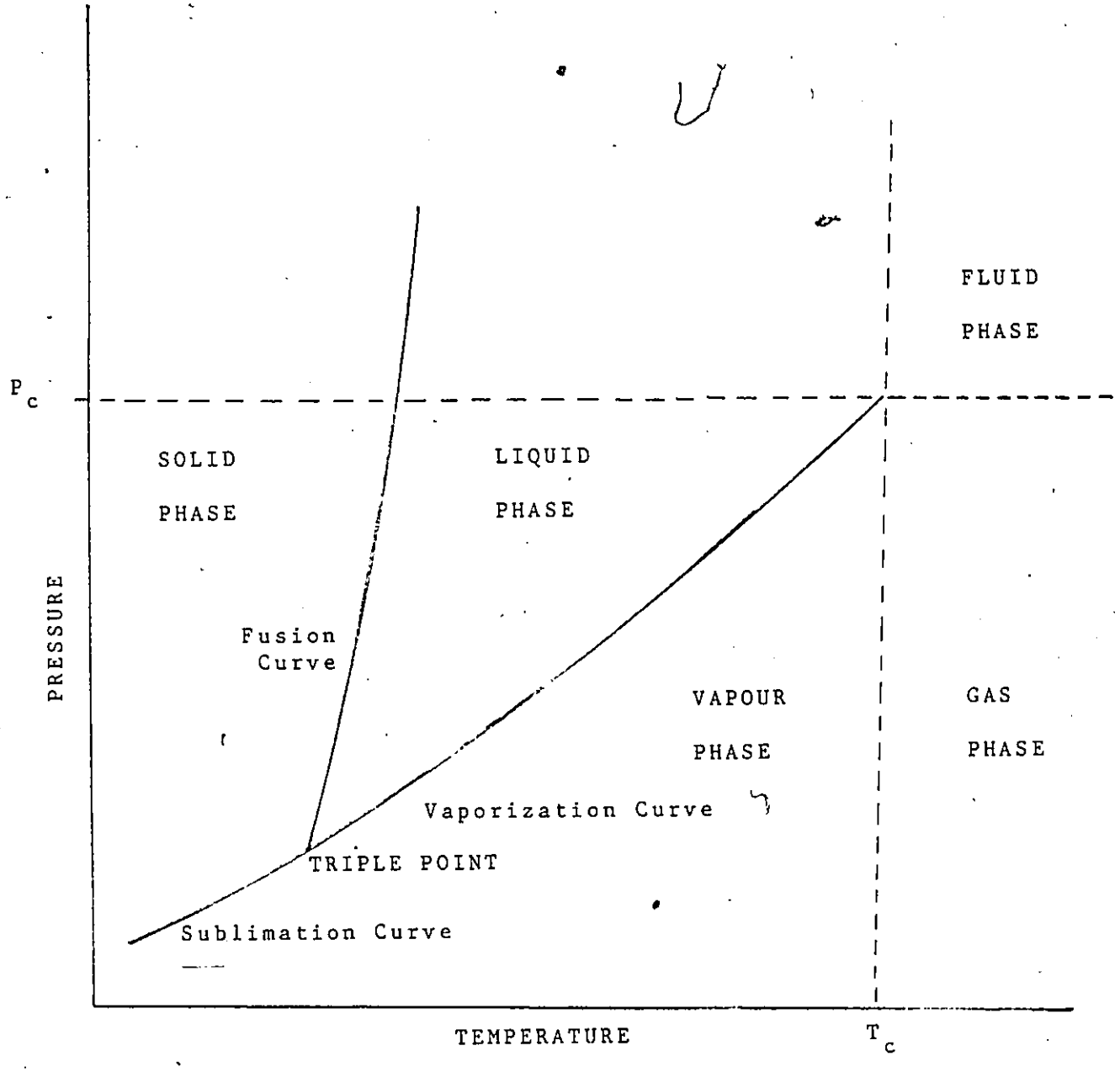

Figure 1: PHASE DIAGRAM FOR A PURE SUBSTANCE

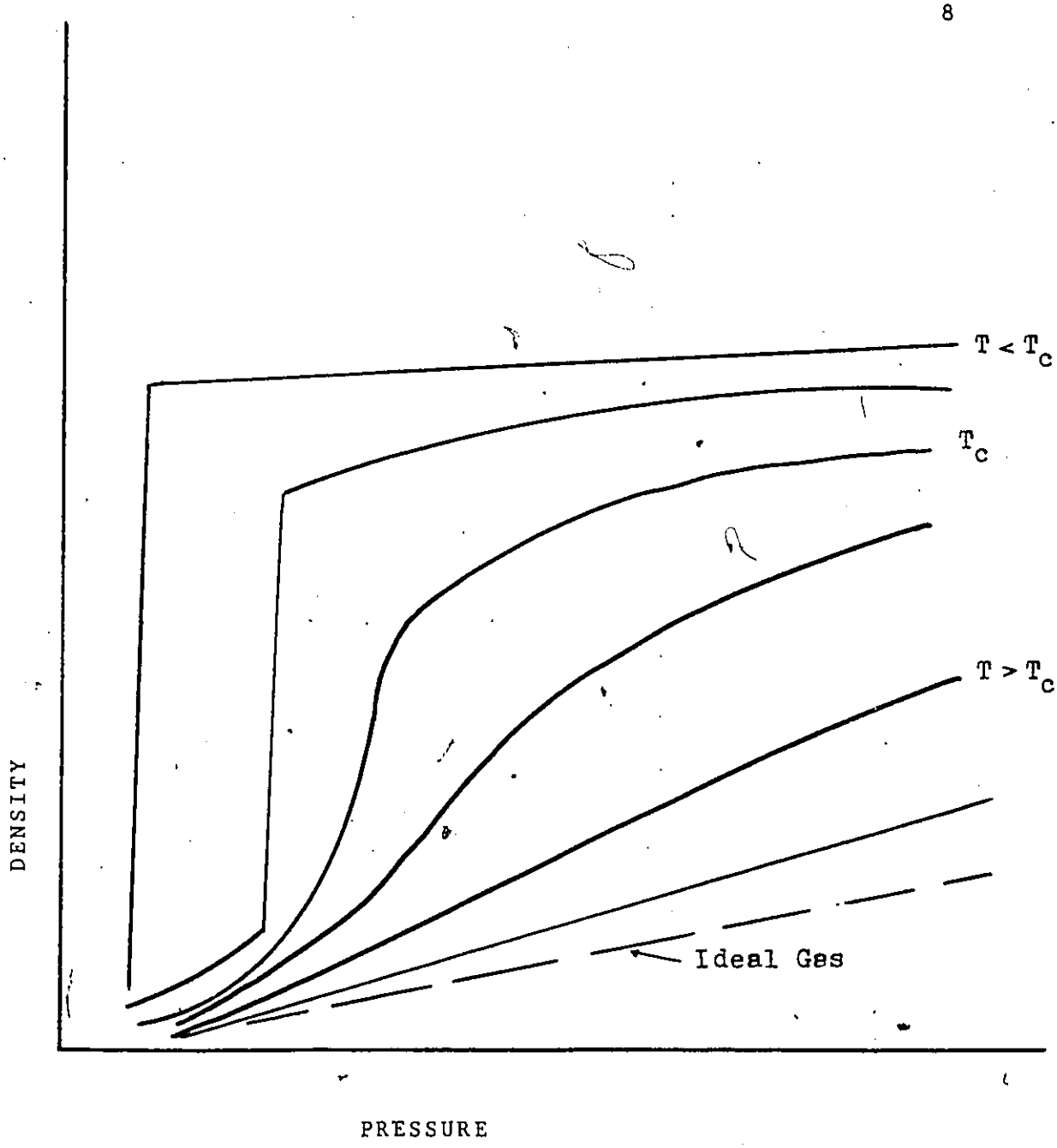

Figure 2: EFFECT OF PRESSURE ON DENSITY FOR PROPANE (3)

supercritical fluid, all of these factors may be manipulated through precise control of temperature and pressure. Increasing the temperature will decrease the density, while manipulating the pressure allows control of both density and the influence of the di-electric constant.

Figure 2 shows the effect of pressure on the density of propane for various isotherms. At very high temperatures, propane exhibits near-ideal behavior. Near or at the critical temperature however, pressure can be seen to have a marked effect on the density. As the density increases, the solubility of less volatile components in the gas generally increases. According to the measurements of Hubert and Vitzthum (3), the extraction rate with supercritical carbon dioxide is at least 2.5 times as high as with the liquid.

The influence of temperature on the solvent properties of the medium can vary. In experiments with napthalene and anthracene, Johnston found that solubility decreased with temperature at low pressure, while the opposite held true at high pressure (4). This would suggest that the degree of solvation in the fluid phase is more dependant on the number of solvent molecules surrounding the solute (i.e. the density) than the pressure. Solubility versus density plots were found to exhibit more regular behavior than pressure plots.

From Figure 2, it is apparent that high reduced

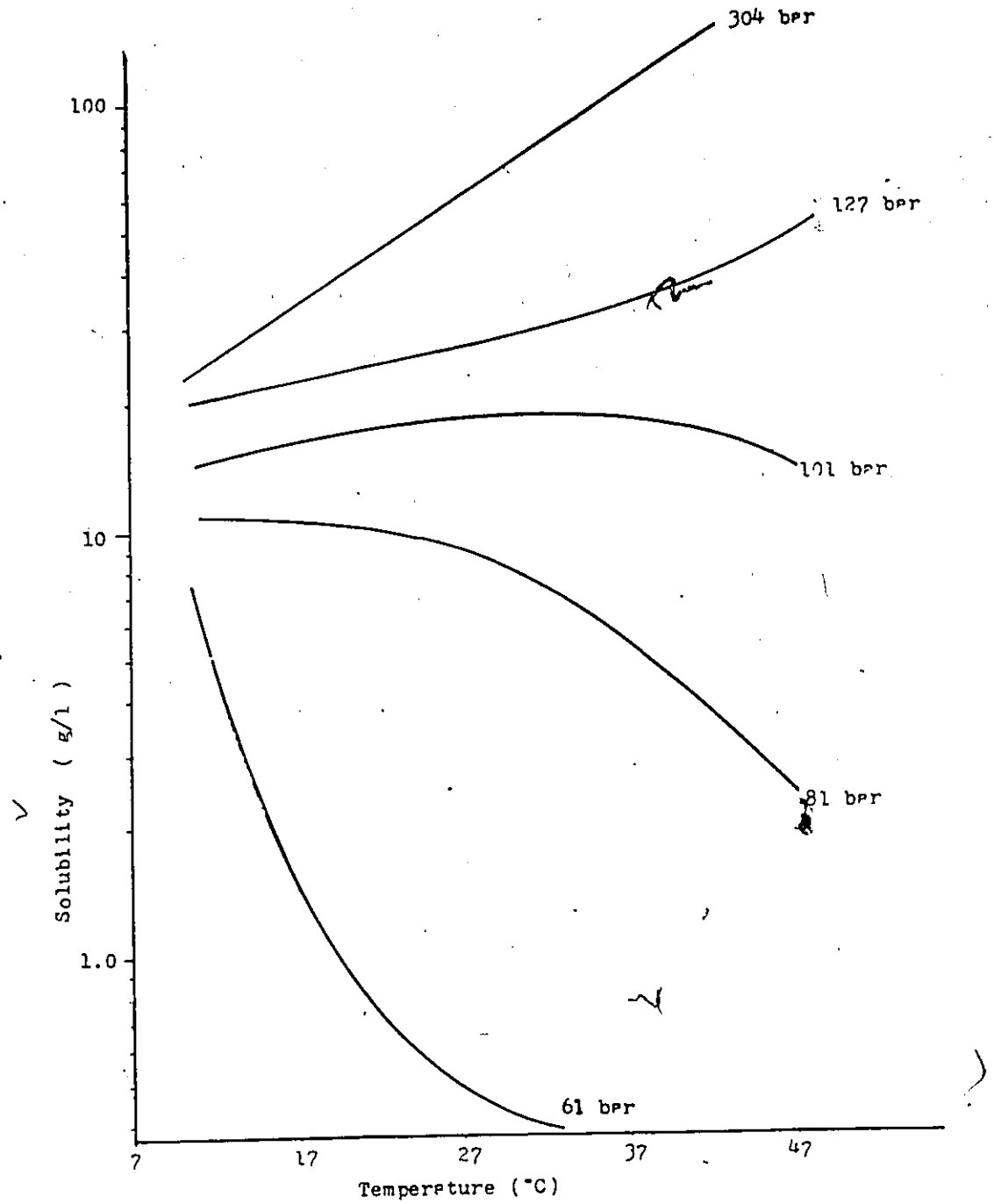

Figure 3: SOLUBILITY OF NAPTHALENE IN COMPRESSED ETHYLENE

(1 bar = 0.1 MPa)

temperatures result in gas-like densities, and we may conclude that gases such as nitrogen and oxygen would make very poor supercritical solvents at room temperature. In Figure 3, we can see that increasing the temperature at higher pressures results in an increased solubility of napthalene in compressed ethylene, while at lower pressures the temperature is inversely related to the solubility. This is the result of competing temperature effects: the vapour pressure of the solute, and the density of the fluid. The more dense the fluid, the greater will be its ability to transport the solute. Density is far more sensitive to temperature in the low pressure region, as was illustrated in Figure 2. At low pressure, this density decrease overshadows the vapour pressure effect, leading to a negative solubility-temperature slope.

At high pressures, however, the vapour pressure effect dominates. The explanation for this lies in the fugacity of the solid solute. As the pressure increases, the fugacity of the solute increases. This leads to a corresponding increase in the volatility in the gas phase.

Phase Behavior

Phase diagrams have proven vital in the study of the behavior of supercritical mixtures. They represent perhaps

the most complex aspect of SCF studies, for specific fluid mixtures may exhibit very different types of phase behavior. However, for all but the most common solvents there is a lack of the necessary data for the construction of a phase diagram. Phase diagrams are crucial for the prediction and understanding of fluid behavior in the supercritical region, and a great deal of current research in the field is directed towards abating this deficiency.

Figure 4 shows the three-dimensional p-T-x surface and its accompanying P-T projection for the liquid-gas phase equilibria of a binary mixture in the simplest case. The dotted lines represent the vapour pressure curves of the pure components a and b, corresponding to x = 0 and x = 1 respectively. The vapour pressure curves end at the critical points CP1 and CP2. Beyond these points, or beyond the curve connecting the two points shown in the projection, the mixture is in the supercritical phase. This curve may exhibit a maximum or minimum, depending on the interaction of the components of the mixture.

At conditions beyond this defining curve the components of the mixture are miscible in all proportions. Thus, for fluid extraction operating at conditions of temperature and pressure beyond this curve, substances can be dissolved completely in the supercritical solvent. For recovery of the solute, a heterogeneous region of the

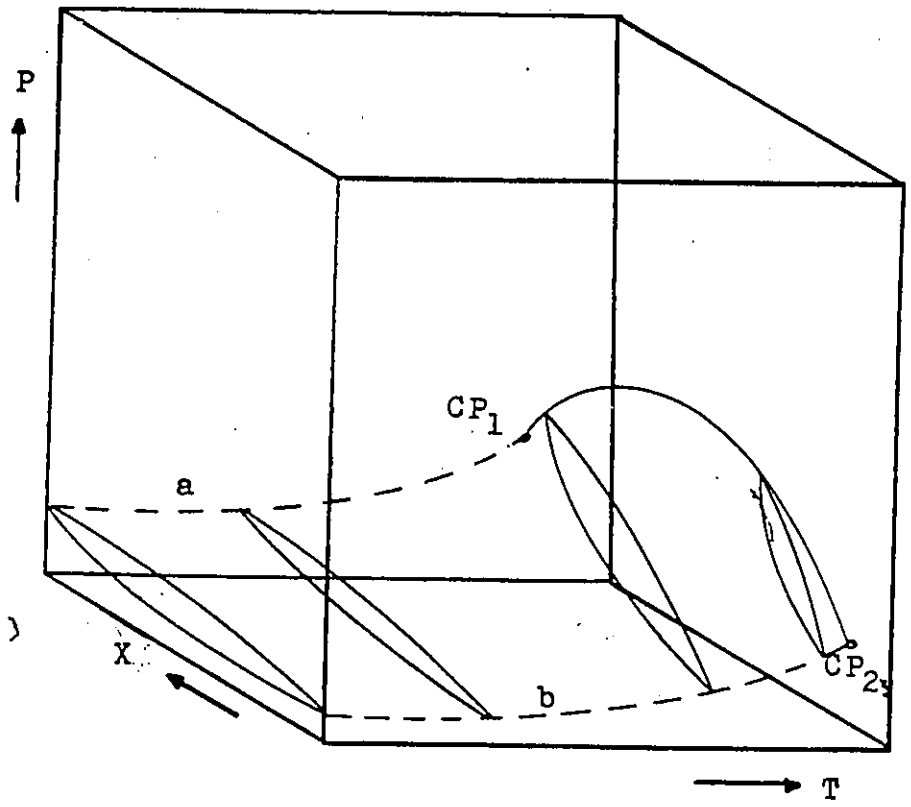

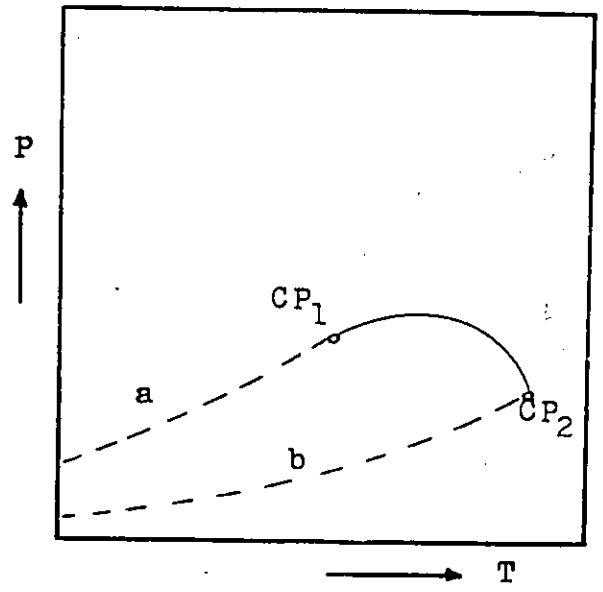

Figure 4: PHASE EQUILIBRIA DIAGRAM FOR A PURE SUBSTANCE AND P-T PROJECTION

diagram must be entered.

Schneider describes a wide variety of phase diagrams in great detail (5). Few mixtures behave in the ideal fashion shown in Figure 4. The components may separate into two liquid phases at low temperatures, necessitating the addition of another surface to the diagram. As the mutual miscibility of the components decreases, the p-T-x surface deviates further from the ideal case. As the liquid-liquid immiscibility line shifts to higher temperatures, it may intercept the liquid-vapour critical locus that connects the pure component critical properties, as happens with systems such as carbon dioxide-hexadecane. As the miscibility continues to decrease, the phase boundary may begin at the critical point of the heavy component, and the system may exhibit gas-gas immiscibility.

Phase diagrams are generally classified according to the appearance of their P-T projections, as shown in Figure 5 (11). The simplest binary fluid systems are class I, which occur in mixtures of similar components. If there is a difference in molecular size or polarity, a class II system may result, where a three-phase liquid-liquid-gas (LLG) coexistence line exists below the vapour pressure curve of the light component. The LLG line terminates at the upper critical end point (UCEP). More significant differences between the components results in a class III system, where

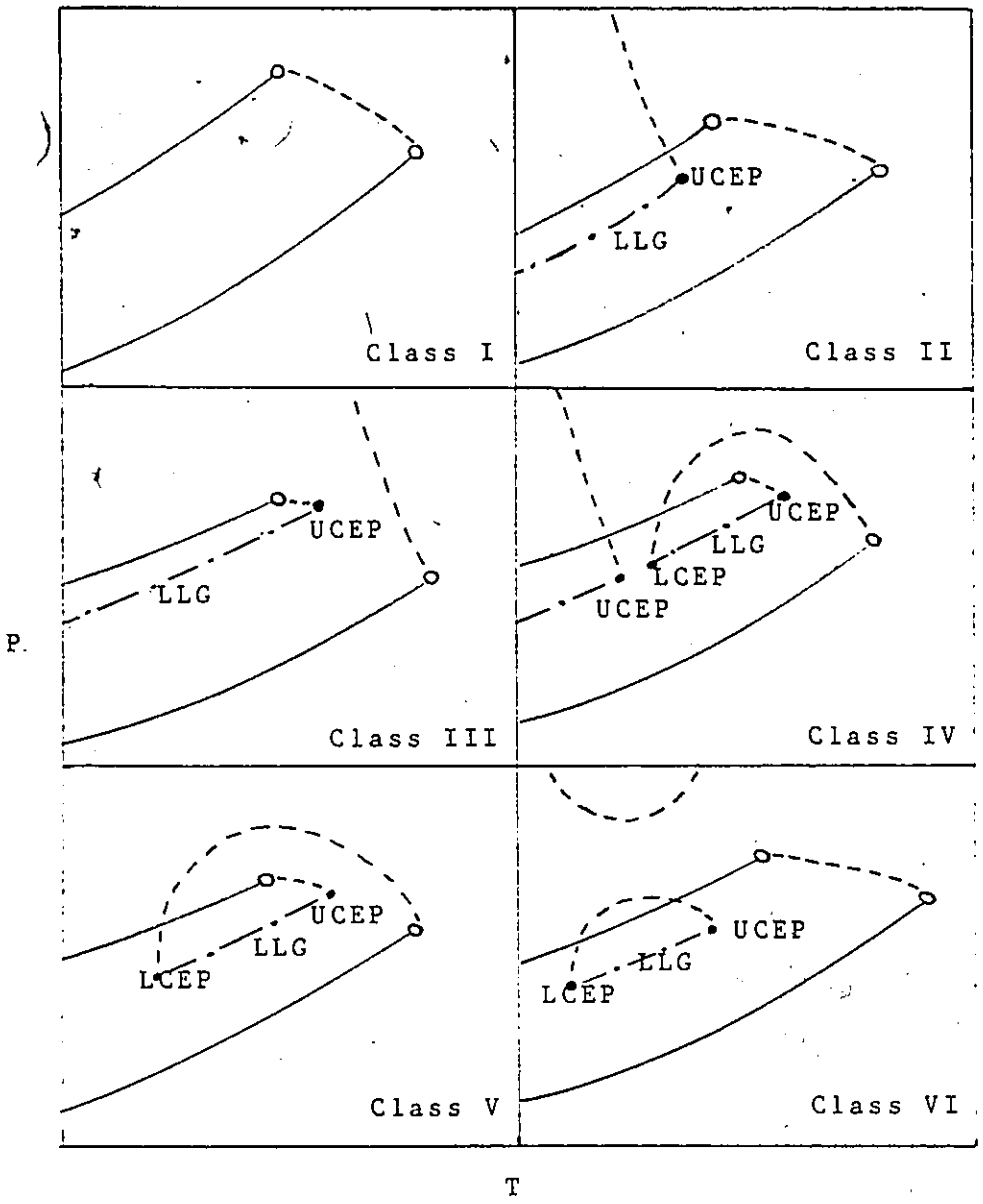

Figure 5: P-T PROJECTIONS FOR BINARY FLUID SYSTEMS

the LLG line cuts the gas-liquid critical locus into two branches.

Very large size or polarity differences can result in class IV systems. The LLG line is now cut by the gas-liquid critical locus, which connects a lower critical end point (LCEP) with the critical point of component 2. A second UCEP exists at the end of the lower branch of the LLG line. If this lower branch is absent, a class V system results.

If the UCEP and LCEP are connected by the liquid-liquid critical locus the system is labeled class VI. Class VI occurs only in certain aqueous mixtures. A second liquid-liquid critical locus exists above tne first, i.e. a region of two immiscible liquid phases exists at high pressures.

Applications of Supercritical Fluid Extraction

While the advantages of using a SFE process may seem attractive, one must be prepared to examine the capital cost of an industrial scale unit. A SFE process is necessarily a high pressure system, and therefore costly. Further disadvantages inherent with such a system include potential safety hazards as a result of high pressure, and the necessity of storage facilities for the large quantities of compressed gas that will be required for most industrial

applications.

These disadvantages are for the most part offset by the simplicity of the process, however. The major components of any supercritical process are fluid circulation compressors and high pressure desorption vessels. The capital cost for these items is less than, for example, that for a multiple-hearth furnace or the associated air pollution control equipment used in conventional systems (2). Extraction pressures in the range of 80 - 300 atmospheres are usually required to achieve adaquate densities for good solute transport, and this is the range that has been most thoroughly investigated. While the occurrence of further dissolution phenomena at higher pressures should not be excluded, it is doubtful that economic factors would permit their use.

Operating costs, as well, are often less than for traditional techniques, specifically in regard to energy requirements. When the compression ratio for recycling the solvent is not too high the energy requirement is significantly reduced from the conventional method of evaporating the solvent. Vaporizing and condensing fluids near the critical point requires little energy as the heat of vaporization at this point nears zero.

In general, extraction with supercritical fluids offers two major advantages over liquids: the solutes are

generally much more soluble, and there is a wider range of operating temperatures. Additionally, the ability to vary the solvent power of the medium as desired within certain ranges without having to change the composition of the solvent, as would be required with traditional solvent extraction, offers a further advantage. This manipulation is achieved through the use of temperature and pressure as process parameters.

As Figures 2 and 3 demonstrate, the solubility of a supercritical solvent is highly dependent upon temperature and pressure, and a change as small as 20° C can result in a change of solubility in excess of one order of magnitude. The selective manipulation of temperature and pressure can achieve specific dissolution or separation effects at relatively low cost. This suggests a number of basic separation schemes, all of which take advantage of this capability, as shown in Figure 6 (3).

The first of these methods is shown in diagram A. This system uses pressure to manipulate the solvent power of the supercritical gas. The basic components of the system are two pressure vessels, one containing the loaded organic phase and the other the separation chamber, a compressor and an expansion valve. In the extraction step, the soluble components of the mixture are dissolved by the supercritical gas. The charged homogeneous phase, essentially a solution,

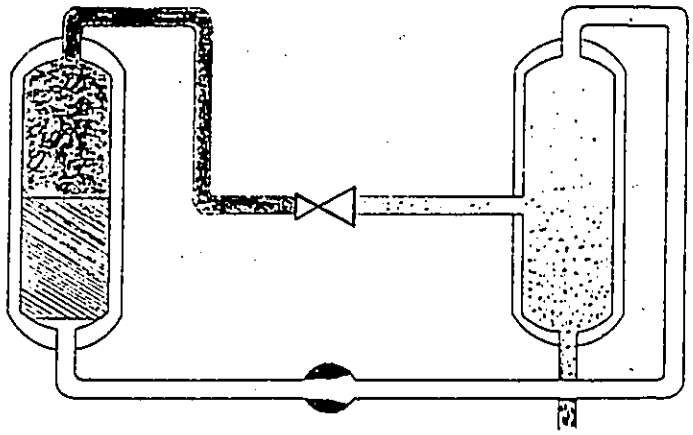

(A) SOLUBILITY CONTROL USING PRESSURE

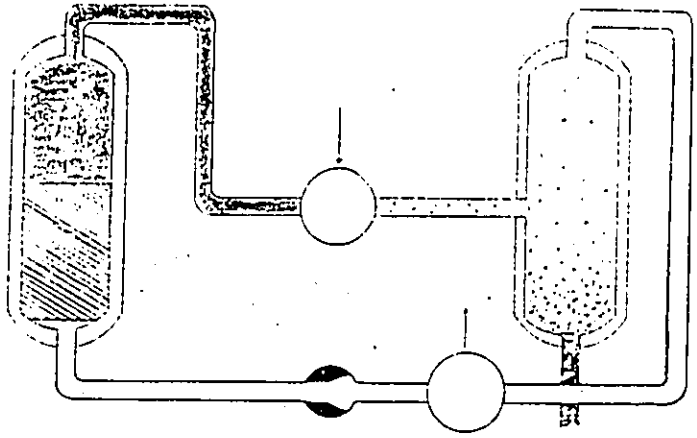

(B) SOLUBILITY CONTROL USING TEMPERATURE

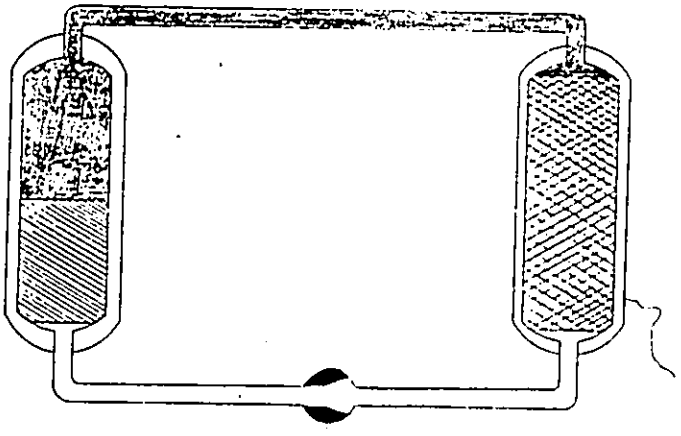

(C) SCF EXTRACTION WITH ACTIVATED CARBON

Figure 6: EXTRACTION USING SUPERCRITICAL FLUIDS

is then decomposed as it passes through the expansion valve into the separation chamber. Here the density of the solvent decreases, and the extract drops out of the fluid phase. The extract is removed and the gas is recompressed and returned to the extraction stage.

A very similar process uses temperature to manipulate the solvent instead of pressure (diagram B). Here the solvent temperature is raised to increase its solubility before it is fed into the separation vessel, and then reduced once the solution has been obtained, with the same results. The advantage here is a constant pressure system, with a minimum of recompression work required.

A third variation of the process is shown in diagram C of Figure 6. Here both pressure and temperature are kept constant, with the solute being removed with the help of activated carbon or a similar absorbant. This process is generally used when it is the carrier (i.e. bulk) substance, not the solute, that is required (e.g. tobacco or coffee).

Extraction with supercritical fluids has been applied to a number of chemical processes, among them deasphalting petroleum stock, the regeneration of spent activated carbon, and coffee decaffeination. Modar Inc. (6) has completed a prototype unit that uses supercritical water to wet-oxidize up to 25,000 gallons per day of hazardous organic wastes. Many organics normally water-insoluble become highly soluble

in the supercritical phase. The water also acts to reform some complex organic pollutants, and many heteroatoms (such as halogens, phosphorus, sulfur, and metals) are precipitated as salts. The unit has a capacity of 500,000 gal/day of water, and reports an efficiency of 99.99%, even for such problem chemicals as organic chlorides, sulfides, and phosphates. Operating costs for the system are reported to be less than for conventional techniques such as high-temperature incineration, since the process requires no fuel.

Industrially pre-engineered units for such uses as removing organics from wastewater and extracting oils from natural products are already on the market. The system offered by Superpressure Inc. of Silver Springs, Md. (7), can employ a number of solvents: carbon dioxide, water, oxygen, ethylene, propane and propylene.

For food processing applications, carbon dioxide is still the most commonly used solvent. Hag AG (8) in West Germany has developed a process which uses supercritical carbon dioxide to extract caffeine from green coffee beans. The method is a variation of the single-cycle technique illustrated in diagram C of Figure 5. Presoaked coffee beans with an initial caffeine content between 0.7 - 3% are fed into a pressure vessel charged with carbon dioxide at 3200 psi, where the caffeine diffuses out of the beans into the

supercritical solvent. The solvent is continuously recycled to a washing tower where the caffeine is removed with water. After ten hours the carbon dioxide is essentially cleansed of caffeine. The caffeine content of the beans is reduced to as low as 0.02%, well below the required value of 0.08%, and pure caffeine is recovered as an additional product of the process.

Current applications of SFE are not limited to small scale pilot-plant operations, and the potential for future applications is vast and includes the extraction and purification of drugs, and coal liquefaction. In the final analysis however, the choice of separation medium must be made on the basis of economics. The pressure and temperature at which the separation is accomplished are key contributors to the capital cost of any system. Actual separation pressures for SCF extractions, which range from 500 psi to over 3000, depend on the application. An economic tradeoff exists between total recovery of the solute, achieved by completely depressurizing the supercritical solvent, and the cost of repressurizing the solvent for a second pass. If the costs for such a system are not prohibitive, then the process industry is in a position to make use of the advantages offered by a supercritical fluid extraction technique.

Chapter II

RESEARCH OBJECTIVES

The potential for food processing using SFE has been the subject of growing attention in the literature. The attractive properties of supercritical carbon dioxide as a solvent have led to a number of proposals for food processing using carbon dioxide as a solvent. The growing consumer demand for low-calorie foods has led to a search for low fat food products, and as a result interest in the food industry for products with reduced oil content has been high. Experiments utilizing supercritical carbon dioxide to extract oil from peanuts, in the hopes of arriving at an inexpensive method of simultaneously producing a low calorie snack food and a high purity peanut oil, have had only limited success.

The higher porosity and surface/volume ratio of potato chips, however, suggests a greater suitability for SFE. The primary goal of this work was to determine the practicality of extracting vegetable oils from potato chips using supercritical carbon dioxide, and to find the conditions for which such removal was optimized. The research was conducted with emphasis on both minimizing operating costs and maximizing oil recovery. To this end a

factorial design was used in the initial study to find the variables of primary interest, and the effect of the major process variables, primarily pressure and flowrate, were studied in detail. A two-level factorial design involves selecting two values for each of the process variables and conducting experiments at each of those levels, in a precise order, in an attempt to find a linear equation that models the process.

Of chief interest was the question of practicality. In order for the extraction process to be deemed successful, it was necessary for the end result to be a marketable product, i.e. the chip must physically survive the extraction process, retain the texture and flavour desired, and be of sufficient oil reduction to warrant the cost. Experience with coffee extraction has indicated that the process will result in an increase in cost of approximately 12%, or roughly $0.06 per bag of chips. Traditional liquid solvents have proven inadequate for the task, especially when the choice of solvent must be limited to those which exhibit no toxic properties.

The effects of four major process variables were studied, notably temperature, pressure, retention time in the cell, and CO_2 flowrate, in an attempt to optimize both total oil removed and oil recovery. Where possible, attempts were made to model the data to facilitate

solubility predictions beyond the range studied. The cost of the developed procedure would be primarily influenced by the operating pressure and, to a lesser extent, the degree of oil recovery, and these variables were worthy of special attention.

Carbon Dioxide Solvent Performance

Of all supercritical solvents, carbon dioxide is the most well studied. It has been found to be completely miscible with low molecular weight hydrocarbon and oxygenated organics, and is therefore a good solvent for organic oils. In addition, its mutual solubility with water is low. While data in the literature concerning actual vegetable oil solubilities is scant, the properties of CO_2 would seem to make it ideal for the proposed work.

Carbon dioxide is particularly attractive for use in food products. It is routinely encountered in the food industry -- for example, it is used in artificially carbonated soft drinks. It is regarded as an "inert gas", even in the supercritical state, and does not react in any way with food constituents (3). The preferred temperature range for extraction with carbon dioxide is from 33 - 80°C, and therefore it poses no danger of thermally damaging food products. While most researchers are confident that carbon

dioxide is physiologically unproblematic, tests have been conducted to check for residual traces of the solvent in foods processed using supercritical techniques. Zosel (8) used radioactive CO_2 in experimental studies of coffee decaffeination and found no radioactivity in the product coffee.

While gaseous carbon dioxide is ineffective as a solvent for liquids and solids of any kind, at high temperatures and pressures the solubility of organic compounds in it greatly increases. Although carbon dioxide is not a universal solvent under any conditions, it is highly selective. It is this selectivity which makes it ideal as an easily controlled extraction medium. The following are the general conclusions about the solubilities of liquid CO_2, compiled from the literature (3,4,8,23):

i) Low-to-medium molecular weight oxygenated organic compounds are soluble, including alcohols, esters, aldehydes, ethers and ketones;

ii) Most low-molecular weight non-polar organic compounds are soluble, such as alkanes, alkenes, and other hydrocarbons, including gasoline;

iii) Very low molecular weight polar organic compounds are soluble, such as carboxylic acids;

iv) Solubility of a compound is decreased by the

presence of polar groups such as hydroxyl, carboxyl, or nitrogenous groups;

v) Salts, fatty acids and their glycerides all have low solubility;

vi) The solubility of water is low: 0.1% at 20°C;

vii) Alkaloids are insoluble in liquid CO_2, but some are soluble in the supercritical phase;

viii) Inorganic and fruit acids are insoluble, as are chlorophyll, sugars, amino acids, and carotenoids.

The low solubility of water and salts is reassuring, for it indicates that substantial changes in the taste and texture of the chips should be prevented during the extraction process. The bulk portion of the chip, composed mainly of carbohydrates, should remain insoluble in carbon dioxide and should not be entrained by the process.

While the oil may be considered essentially tasteless when it is introduced during the frying stage of chip production, this should not be considered the case in the final product. To what degree the oil may be removed from the chip before it begins to suffer in terms of taste and texture must also be resolved.

The degree of oil removal from the chip necessary for a significant reduction in the calorie content is not high. The average potato chip contains from 35 to 37% oil by

weight (9), but it is this component that accounts for the majority of the calories in the final product. Typical vegetable oil caloric value is approximately 9.3 cal/gram, while that for the remainder of the chip is less than half this value, 4.1 cal/gram (10). Thus, a reduction in total chip weight of approximately 33% will result in a drop in total caloric value of over 50%. While the demands of taste and desirability for the final product may place limits on the total amount of oil which may be extracted from the chip, the potential for substantial reductions in the total calorie content of the final product exists.

The choice of operating region for the experiments is an important one, for narrowing the range of temperature and pressure which needed to be investigated resulted in a substantial savings in time and expense. In order to locate those regions most suitable for investigating the solubility of oils and similar substances in supercritical carbon dioxide reported in the literature were studied.

Filippi (12) extracted vegetable oil from several types of oil seeds using carbon dioxide, and his results are shown in Figure 7. At a temperature below the critical point (20°C), solubility increases until a pressure of the order of 300 atm and then remains fairly constant. Solubility values for this isotherm are in the range of 0.2 to 1.0 per cent by weight. For the 55°C isotherm the solubility rises

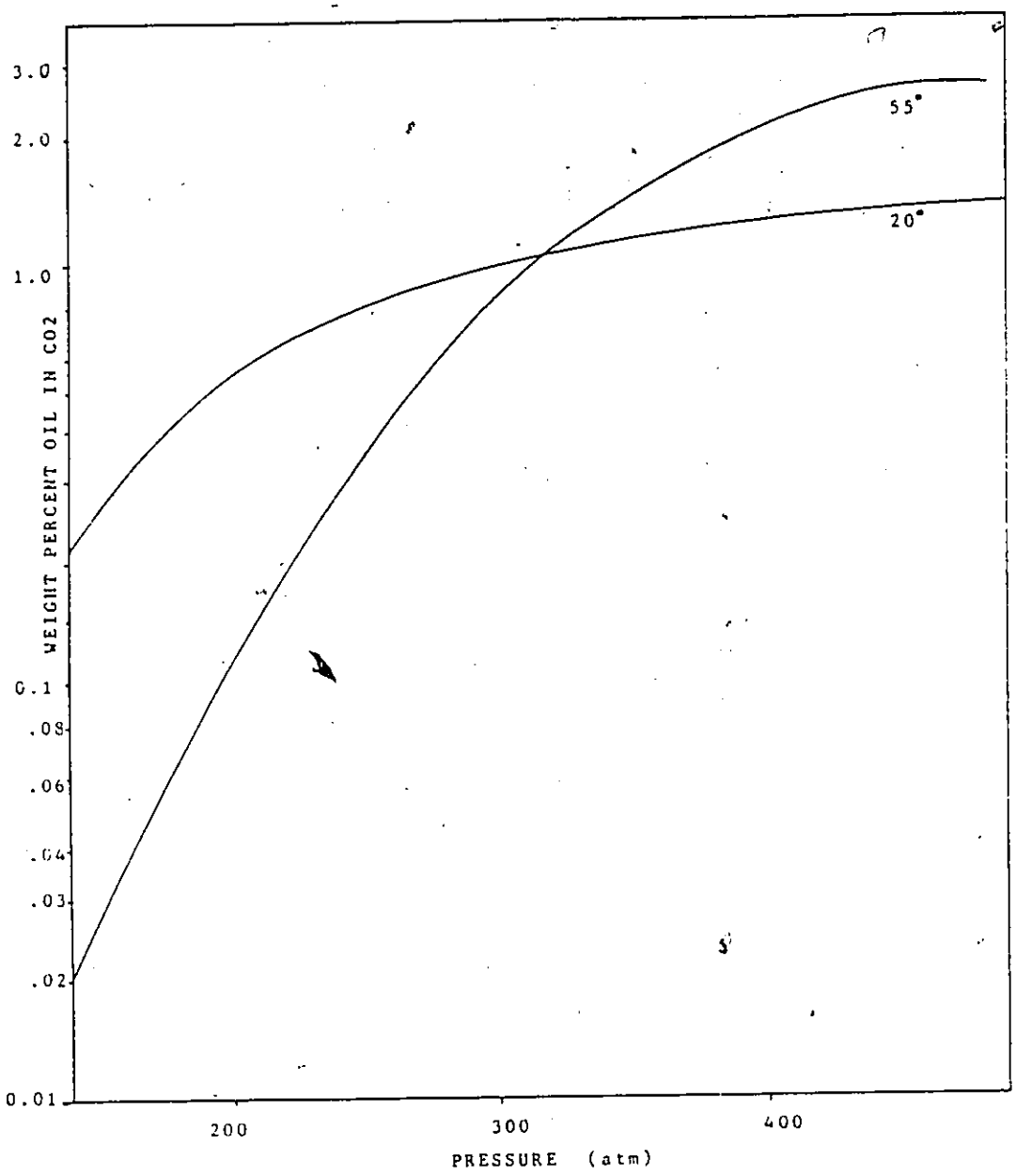

Figure 7: SOLUBILITY OF VEGETABLE OIL IN CARBON DIOXIDE

much more rapidly, and this trend continues throughout the range shown. The high-pressure solubility values are greater than those shown for the lower temperature, but the solubility values below 300 atm are lower than the corresponding levels at 20°C. Thus, there is an inversion of the solubility-temperature relationship with pressure. The solubilty range for the high temperature isotherm is from 0.02 to 3.0 per cent.

This plot serves to show the complexity of the P-T-x response surface for oil solubility in supercritical carbon dioxide. The two curves in the figure may be considered as two P-x projections of a phase diagram; the region between the two isotherms (i.e. the behavior of the surface between 20° and 55°C, when carbon dioxide crosses the critical point) remains unknown. An added complication arises when vegetable oil is treated, not as a pseudo-pure component as it is here, but as a complex mixture of many fats of unknown composition and distribution. Such a mixture requires an n-dimensional phase diagram, where n represents one greater than the number of components. Since vegetable oil can consist of hundreds of components, and changes in composition seasonally as sources fluctuate, such a treatment would require an inordinate amount of data and must be considered unrealistic.

More recently (24), studies have been made of

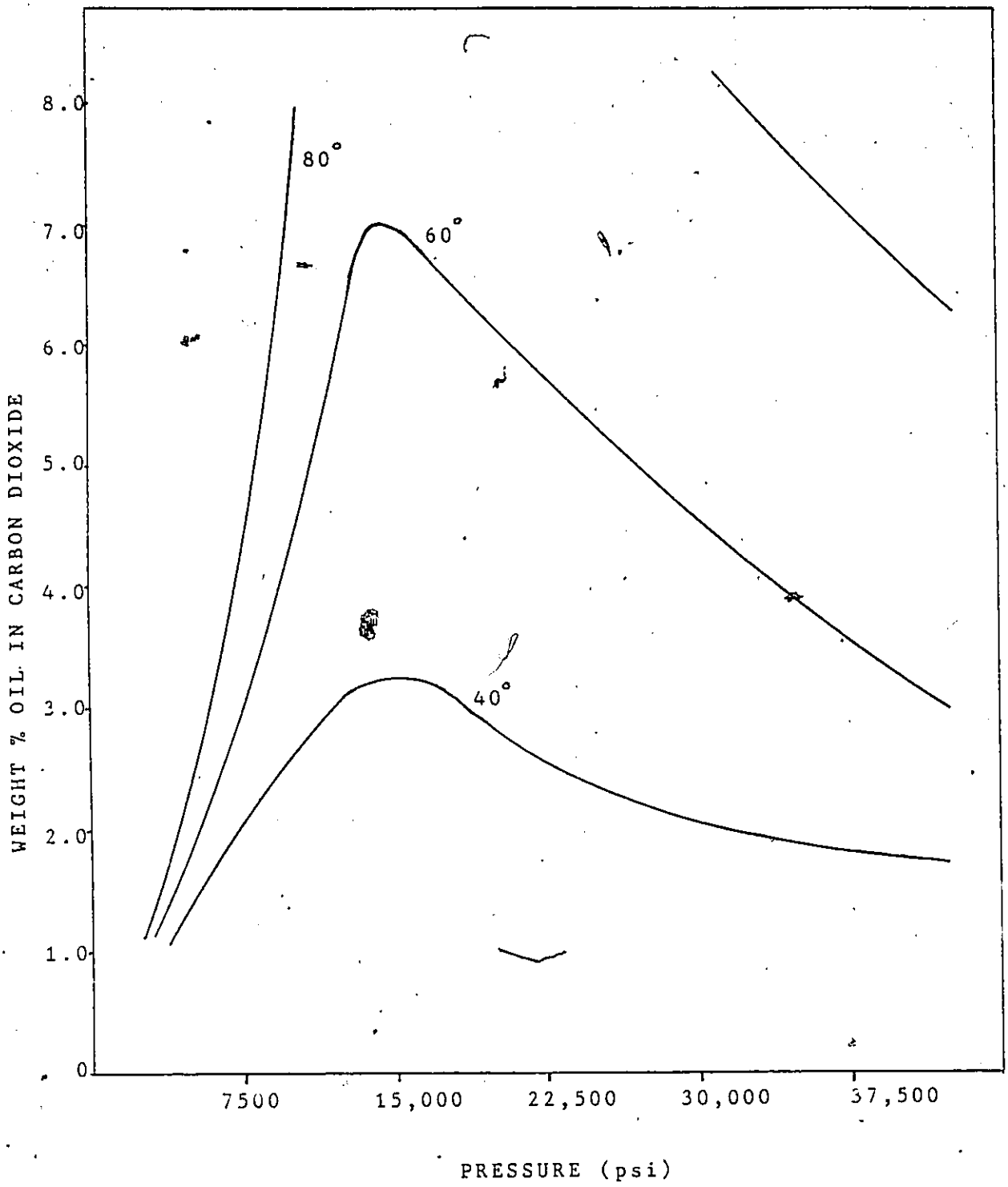

Figure 8: SOLUBILITY OF SOYBEAN OIL IN SUPERCRITICAL CO2

extractions of "pure component" oil (i.e. an oil derived from a single source). One such plot is shown in Figure 8, the solubility of soybean oil in supercritical carbon dioxide. Here the response surface exhibits more regular behavior, and the P-x projections display increasing solubility with increasing temperature. The choice of suitable operating regions for extraction is more obvious from this plot.

Both Figures 7 and 8, however, share the disadvantage of inadequate pressure range. The lowest point on the graph in Figure 8 is more than twice the operating pressure of the coffee treatment previously discussed. Unless oil recovery were to prove very high, the cost of operating in this region would be prohibitive, both in terms of capital investment and recompressing the solvent. Neither Figure 7 nor 8 shows the solubility of oil in the region near the critical point. While extrapolation of the curves would indicate that solubilities would be low in this region, experience has shown that behavior at the critical point is very difficut to predict in this manner. Since operation near the critical point would result in the lowest operating cost for the process, this region is worthy of investigation.

Solubility Prediction

The major stumbling block in the development of supercritical fluid technology as a viable alternative to conventional extraction techniques has been the substantial absence of data. While numerous applications for SFE processes have been proposed, data for all but the most common systems is sorely lacking. The bulk of present research is aimed at qualitatively and quantitatively describing solubilities, with the hope of using this information to define a theoretical model of the supercritical state. Ultimately, with the help of such a model and the construction of phase diagrams for more complex systems, such research should result in reliable predictions for the solubility of a solute in a supercritical phase.

For the time being, attempts to describe these solubilities are constrained to two approaches: the use of an expression directly relating the concentration of solute to a solubility parameter or density of the extraction fluid, and the use of an equation of state. The more traditional approach is the use of an equation of state. However, in the supercritical region these equations often fall short of the required accuracy. For a binary or multi-component system, this inaccuracy is compounded by

empirical mixing rules.

In order to evaluate the dissolving power of a supercritical gas, it is necessary to determine its phase equilibria with the solute. However, in some cases even this is not sufficient, as in the case of some vegetable products, since the way in which the substance to be extracted is bound to the vegetable matrix has a considerable influence. The extraction of nicotine from raw tobacco is one such case: whereas some of the nicotine may be easily removed by extraction, some remains in the tobacco as a complex salt with chlorogenic and citric acids, and is more difficult to remove. There are many parameters to be considered before a process is designed, and while the behavior of less complex systems may be predicted with some confidence, there is no substitute for actual data.

In the absence of sufficient data or a phase diagram, solubilities must be predicted. The solubility of a solute in a supercritical solvent is most commonly determined from fundamental thermodynamic relationships by equating the fugacity of the solid and fluid phases. In the supercritical region it is common practice to extrapolate the fugacity coefficient to the liquid phase, and the activity coefficient to the gaseous phase. However, this method of fugacity calculation requires the integral of $\overline{V}i\ dP$. Given the scarcity of partial molar data in the supercritical

region, particularly as a function of pressure, the more conventional approach is to treat the fluid as a compressed gas and approximate the fluid-phase fugacity from volumetric properties. The evaluation of the solid-phase fugacity is usually done by the method of Prausnitz (13). Making the assumptions that the solid is pure, incompressible, and has a vapour fugacity coefficient of unity at T and P^{sat}, the equilibrium mole fraction of a solute dissolved in the fluid phase can be evaluated. At moderate pressures, the fugacity coefficient can be calculated using the virial equation of state, as reliable values of second virial coefficients are available. Higher order coefficients are more difficult to obtain however, and empirical equations of state such as the Redlich-Kwong (14) are required for higher pressures.

Since we are interested in a multi-component system, mixing rules will be required for the calculations. Van der Waals one-fluid model (15),

$$a = \sum_i \sum_j y_i y_j a_{ij}$$

$$b = \sum_j y_j b_j$$

and the rules of Prausnitz (16) are commonly used. As with any simplified model, however, the results generated do not

always match experimental data as well as could be hoped. The difficulty in predicting vapour-liquid equilibria for the supercritical region may not be a result of the inadequacy of the equations of state themselves, but rather the use of empirical constants in the equations that were obtained from data collected in the subcritical region.

Solubility data have been successfully correlated on a log-log plot of concentration vs. solvent density. This suggests that solubility may be related to density according to a power law, and that specific chemical forces in the fluid phase are at work. Robin and Vodar studied the solubility of phenenthrene in compressed gases (17), and proposed the following equation to model their results:

$$\text{Log } m = A + Bd \qquad (2.1)$$

where m represents the mass of the solute in g/cubic cm of the compressed gas, d is the gas density, and A and B are constants. This equation was developed using a virial equation of state limited to the second virial coefficient. Stahl et al. (18) proposed the following equation, valid for a wide variety of substances over a pressure range of 80 to 2000 atm,

$$\ln c = m \ln d + k \qquad (2.2)$$

where c is the concentration of a solute in the supercritical fluid and k is a constant. Both the constant k and the factor m vary with the properties of the solute.

From the association laws and the entropies of the components, Chrastil (19) derived

$$c = d^{k} \exp (a/T + b) \qquad (2.3)$$

where c is concentration of solute in g/L of fluid; d also has units of g/L; and a, b and k are solubility constants. Rearranging equation 2.3 gives

$$\ln d = k^{-1} (\ln c - (a/T + b)) \qquad (2.4)$$

This relationship was found to be linear up to relatively high solute concentrations, from 100 to 200 g/L. Adachi and Lu (20) modified the Chrastil equation to improve its capability of data representation by considering the quantity k to be density dependent. In an overall evaluation of several equations of state, they found the Chrastil equation to give a better representation of solubility data from the literature. It was this equation which was chosen to model our data.

Chapter III

APPARATUS AND PROCEDURE

This section outlines the experimental aspects of the research, including the design, planning and execution of the data collection. Two different techniques were used during the first two stages of experimentation: a batch (or static) method was utilized while the runs outlined by the factorial design were conducted, and a flow method was used in the second stage of experimentation. Stages one and two were required to find the variables of primary interest and study the effects of the important process variables in detail, respectively. The third and final stage of data collection was concerned with a qualitative analysis of the survivability and marketability of the final product, potato chips of reduced oil content.

A schematic of the basic apparatus is shown in Figure 9, and a more detailed cutaway of the equilibrium and expansion cells is given in Figure 10. The apparatus was simple in both design and operation, involving only two cells and a single avenue of flow for the supercritical solvent. A detailed description of the apparatus follows, with letter codes for the equipment as given in Figure 9.

Compressed carbon dioxide gas at a pressure of approximately 800 psi is supplied from a cylinder (A)

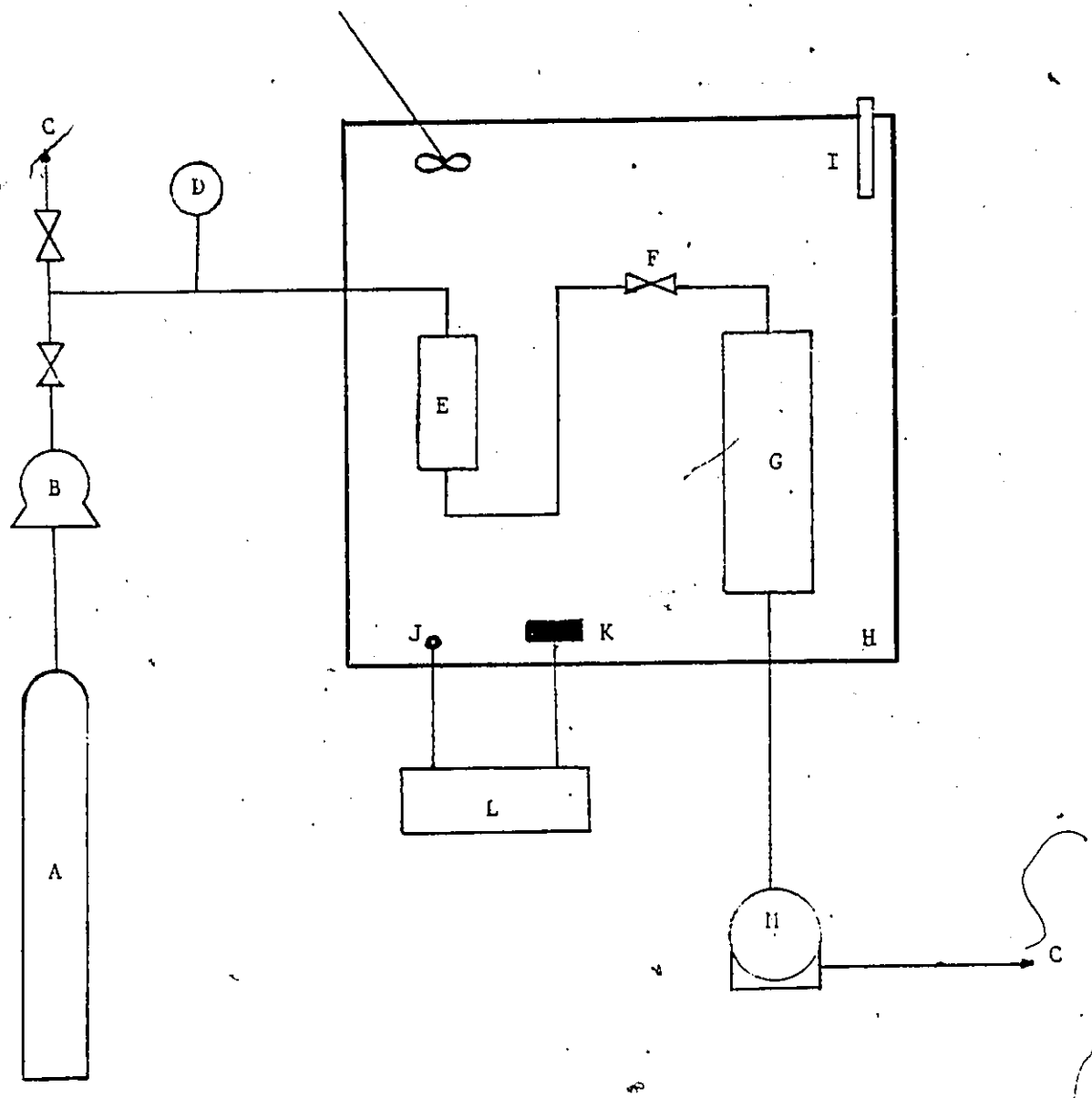

Figure 9: SCHEMATIC OF SYSTEM DESIGN

A: Gas Cylinder; B: Booster Pump; C: Purge to Atmosphere; D: Pressure Transducer; E: Equilibrium Cell; F: Expansion Valve; G: Expansion Cell; H: Constant Temperature Bath; I: Thermometer; J: Temperature Probe; K: Heater; L: Temperature Controller; M: Wet Test Meter.

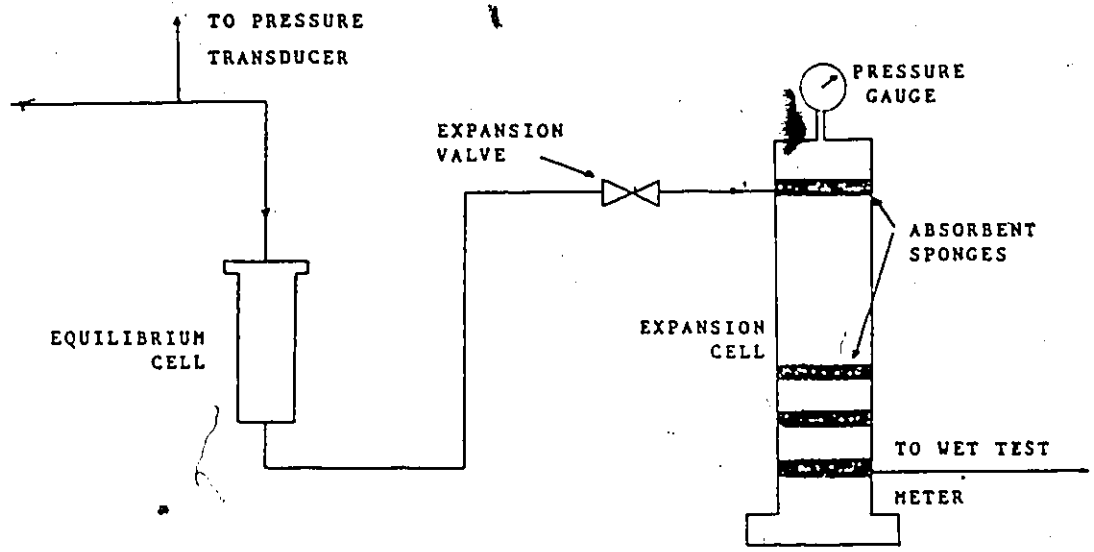

EQUILIBRIUM CELL

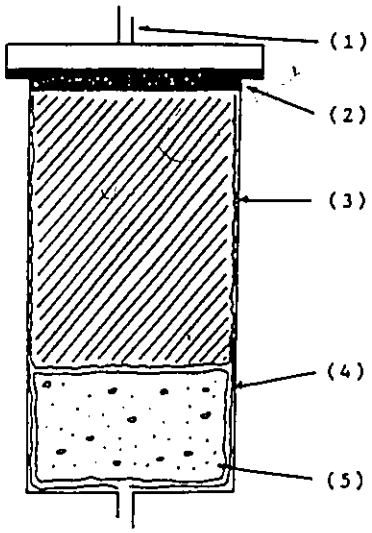

KEY:

1) CO2 INLET
2) TEFLON GASKET
3) NYLON CONTAINER
(CONTAINING CHIPS)
4) PLASTIC ENVELOPE
5) ABSORBENT SPONGE

Figure 10: EXPERIMENTAL APPARATUS

equipped with a dip-tube. Gas pressure is intensified to the desired level through the use of the booster pump (B). The pump is a Futurecraft model 90970 automatic pressure intensifier. It consists of two cylinders connected by a differential area piston. Compressed gas is supplied through a hand loading pressure regulator to the large diameter cylinder. The resulting piston movement compresses the gas to the small diameter cylinder. When the piston reaches the limit of its stroke, the gas in the large cylinder is vented and the cycle is repeated. Outlet pressure is approximately ten times the supply pressure, to a maximum of 5000 psi (34.2 MPa).

Compressed gas in the supercritical state passes through a two-way valve to the equilibrium cell (E). A purge valve leading to the atmosphere is located on this line (C), as well as the pressure tranducer (D) used to indicate the pressure within the cell. The pressure transducer is a Sonotek Model SA, accurate to + 0.05% (see Appendix D for calibration curve). The valves are Autoclave Engineers SW series non-regulating valves with 11,000 psig (76 MPa) maximum allowable pressure.

The equilibrium cell is a stainless steel cylinder of 18 cm height and 305 ml internal volume, pressure tested to 4000 psi (28 MPa). It contains a precautionary filter, a teflon gasket, and a porous nylon jacket retaining the oil-laden chips, as well as a plastic envelope containing an

absorbent sponge under the chips. Flow out of the equilibrium cell is controlled by an expansion valve (F). Solute-laden carbon dioxide flows through the valve into the expansion cell (G), where the pressure is reduced to a maximum of 30 psi Four sponges absorb the discharged solute. The expansion cell has a height of 54 cm and interior volume of 3800 ml. It is stainless steel, pressure- tested to 100 psi, and equipped with a pressure gauge.

Both experimental cells are encased in a constant temperature water bath (H), continuously mixed by a constant speed impeller. Temperature in the bath is controlled by an exterior Bayley instrument precision temperature controller, model 250 (L), connected to a temperature probe (J) and submersible heater (K). The temperature in the bath is controlled to within + 0.05 K, and is monitored by a high-precision mercury thermometer (I) to the nearest 0.05 K.

Flow from the expansion cell leads to a Precision Instruments wet test meter (M), and then is purged to the atmosphere. Atmospheric pressure at the time of the run is measured with a mercury barometer. Tubing connecting the system components is made of stainless steel, with a 1/8 in. (3.175 mm) outer diameter, except for the 1/4 in. (6.35 mm) tubing joining the expansion cell.

The materials used in this work are market grade potato chips and carbon dioxide. Potato chips were obtained

from Hostess Food Products, supplied with a single lot number to guarantee consistency of manufacture. The carbon dioxide is obtained from Air Products, with a minimum purity of 99.9%. Acetone is used as a cleansing agent, and is supplied from Canlab with a purity exceeding 99.9%.

The compressibility factor of pure carbon dioxide is required for the calculation of solvent density. This is obtained from the high precision equations of state developed by IUPAC (21,22). Appendix B summarizes the equation and gives a FORTRAN program used for the calculation of the compressibility factor. The balance used for all weight measurements was a Mettler Model H20, accurate to + 0.00002 g.

Experimental Design

In the first stage of experimentation a two-level fractional factorial design was used to find the primary variables of interest from the four variables selected as possibly significant. Experiments were conducted over a narrow range of pressure and temperature, where the slope of the response function could be approximated as linear. The defining relation chosen was:

$$I = X1X2X3X4$$

which led to the alias structure:

$$X12 = X34; \quad X13 = X24; \quad X14 = X23$$

The coded variables were:

		HIGH (1)	LOW (-1)
TEMPERATURE	(X1)	38.0°C	33.0°C
PRESSURE	(X2)	1120 psi	1070 psi
PURGE RATE	(X3)	FAST	SLOW
RETENTION TIME	(X4)	8 HOURS	24 HOURS

The runs were randomized and organized according to the structure shown in Table 2. Replicates were done to obtain an estimate of the sample variance. An analysis of a least squares fit of the data would indicate those variables which influenced the total oil removal to the greatest extent, as well as ascertaining the existence of any interaction terms between the process variables.

In the second stage of experimentation the variables of chief influence to the cost of the process, pressure and flowrate, as well as the variable of primary importance to oil removal (as indicated by the least squares fit), retention time, were studied in detail. The responses observed were oil removal and oil recovery, factors of considerable importance in the evaluation of practicality.

Table 2: RUN ORDER FOR FACTORIAL DESIGN

TEMPERATURE	PRESSURE	PURGE RATE	RETENTION TIME	RUN#
-1	-1	-1	-1	3,9
1	-1	-1	1	4
-1	1	-1	1	1,6
1	1	-1	-1	10,11
-1	-1	1	1	8
1	-1	1	-1	5
-1	1	1	-1	7
1	1	1	1	2

The results were fitted to a model in an attempt to facilitate prediction of the responses beyond the ranges studied, and were further used to locate the optimum operating region, i.e. that region for which oil removal and recovery were optimized, and for which recompression costs were not prohibitive.

A flow process was used for this phase of the experiment, and the apparatus was slightly modified to facilitate the change in procedure and to implement improvements suggested by the results of the first stage of data collection. The advantages and disadvantages of the two techniques, both in terms of cost and effect on the response variables, were compared in the final analysis.

The last stage of experimentation was concerned with the effect of the process on the marketability of the chips. The taste and texture of the extracted chips were compared qualitatively to untreated chips in a double-blind taste test. To facilitate analysis of the results the test was conducted over two separate days, and an estimate of the reliability of the testing procedure was obtained by comparing the responses of those individuals who took the test on both days. A chromatographic analysis was performed on both the unextracted and recovered oil to determine if fractionation of the oil occurred during the extraction stage.

Batch Method

Approximately 35 grams of potato chips are packed into a porous nylon and weighed using the gravimetric balance. The plastic envelope and absorbent sponge are weighed and placed in the equilibrium cell. Four sponge wafers are similarly weighed and placed in the expansion cell. The cells are sealed and connected to the apparatus. The water bath is flooded with water at approximately room temperature and allowed to come to equilibrium at the design temperature.

The system is throughly purged of air. The purge valves (C) and expansion valve (F) are sealed, and the system pressure is slowly increased to the desired value. When the retention time has elapsed, the cylinder is closed and the expansion valve opened, allowing the solute-laden carbon dioxide to flow into the expansion cell and then vent to the atmosphere. Total carbon dioxide flow is measured by the wet test meter. Atmospheric pressure and total purge time are recorded.

The nylon container, chips, plastic envelope, and sponges are weighed, and the total oil removal and oil recovery are calculated. Oil recovery consists of two categories: oil recovered in the expansion cell, and oil trapped in the nylon and absorbent sponge within the

equilibrium cell. The apparatus is disassembled and the major components are washed with acetone and the process repeated.

Flow Method

For the flow method, one significant change was made in the apparatus: the plastic envelope and sponge within the expansion cell were removed in an attempt to improve the oil recovery in the expansion cell. The start-up procedure for the experiment is identical to that outlined above, with the exception that at the end of the retention time the expansion valve (F) is opened only slightly to allow the desired (slow) flowrate, and the cylinder is left open to allow the booster pump to maintain the pressure in the equilibrium cell at the desired level. Pressure fluctuations within the system as a result of the flowrate are kept below 2% by manually adjusting the expansion valve. When the flowrate has stabilized, the process is permitted to run until exactly 10.2 cubic feet (289 L) ± 0.05 cubic feet (1.42 L) of carbon dioxide have been purged to the atmosphere. The expansion valve is closed and the system allowed ten minutes to stabilize. The cylinder is closed and the system purged as above. Oil removal and recovery are calculated, and the process repeated.

Chapter IV

RESULTS AND DISCUSSION

The results of stages one and two of the experiment are summarized in Tables 3 to 7 and plotted in Figures 11 to 15 (discussed below). Raw data is listed in Appendix A. The results of the final stage of experimentation, the qualitative and chromatographic analysis of the product, are also reviewed.

Least Squares Fitted Model

A least squares fit of the data collected during stage one yielded the following model (neglecting third and higher order interaction terms):

$$\hat{Y} = 2.296 + 0.221X1 - 0.076X2 + 0.039X3 + 0.707X4 + 0.148X12 - 0.041X13 + 0.172X14 \qquad (4.1)$$

with a sum of squares of residuals of 5.456. $\hat{Y}$ is the fitted response, oil removed (grams), and X12, X13, and X14 are the confounded interaction terms. A reduced model is arrived at by an analysis of sample variance. From the sample variance we may compose a 95% confidence interval for the parameters

and eliminate those for which such an interval includes zero (see Appendix C). Our reduced model is thus

$$\hat{Y} = 2.296 + 0.221X1 + 0.707X4 \qquad (4.2)$$

From this model we may conclude that the variables of primary influence on the total oil removal are retention time and, to a lesser extent, temperature. Over the range studied pressure and purge rate were concluded to have a negligible effect on the oil removal.

Effects of Flowrate and Pressure

Stage two of the study was concerned with an investigation of the effects of pressure and flowrate on the oil removal and recovery. The variables were studied over a range far more extensive than would have been feasible for the factorial design. The results of the first stage of the experiment were used in the planning of experiments for the flow stage. Since the model indicated that interaction terms between the four major variables were negligible, an analysis of a single variable conducted at constant levels of the remaining variables was considered a valid method of investigation. Since the model indicated that oil removal was chiefly dependent on retention time in the cell, flow experiments were carried out at two levels of retention

Table 3: OIL REMOVED vs. CO_2 FLOWRATE at 306.1 K

The data given in this Table is plotted in Figure 11

FLOW RATE ft^3/min	OIL REMOVED g	RETENTION TIME hrs	RUN#
0.172 ± 0.006	1.947 ± 0.023	22	23
0.118 0.007	1.953 0.023	22	24
0.257 0.008	0.958 0.011	3.5	25
0.382 0.009	0.953 0.013	3.5	26
0.052 0.001	2.663 0.032	22	27
0.061 0.002	1.206 0.017	3.5	28
0.292 0.009	2.236 0.031	22	29
0.136 0.003	1.753 0.023	22	30
0.153 0.005	0.813 0.009	3.5	31
0.168 0.004	0.966 0.013	3.5	32

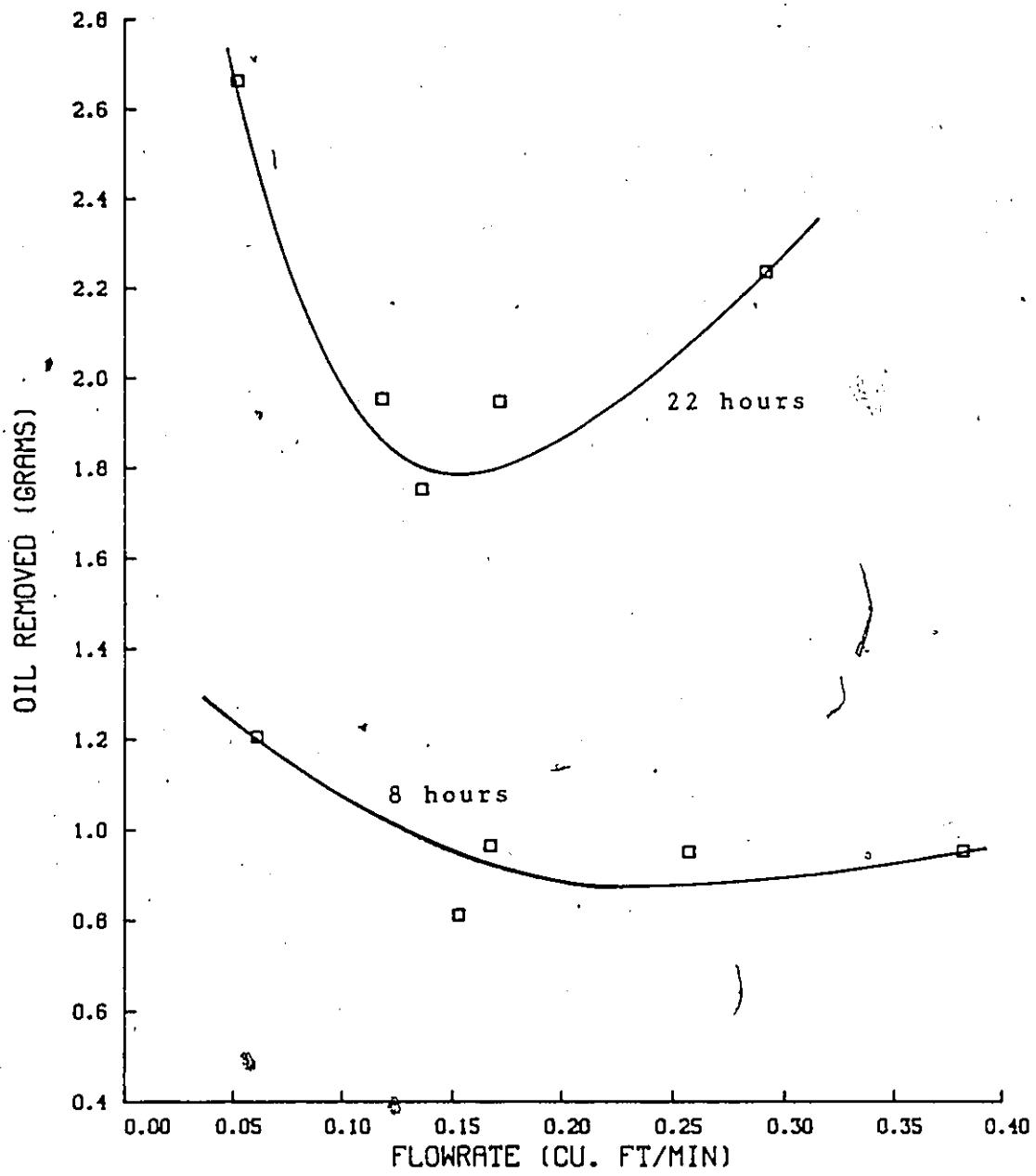

Figure 11: PLOT OF OIL REMOVED vs. CO_2 FLOWRATE

time: 3.5 and 22 hours.

The effect of flowrate on oil removal is plotted in Figure 11, with data given in Table 3. The expected form of this graph was a linear plot of negative slope, since the amount of oil dissolved and removed by the flowing solvent could be expected to be largely dependent on the carbon dioxide residence time in the cell. However, the parabolic shape of both curves would serve to indicate that physical entrainment of the oil occurs with flowrates in excess of approximately 0.15 cubic feet per minute, resulting in a corresponding increase in total oil removal. This entrainment most likely takes the form of the physical movement of oil trapped in the nylon or along the cell wall as a result of frictional forces.

An analysis of the percentage oil recovered outside the cell supports the entrainment hypothesis. The physical entrainment of oils by the supercritical solvent at high flowrates would lead to both a decreased oil recovery within the equilibrium cell and an increased recovery in the expansion cell. The high retention times within both cells permitted by low flowrates would have a similar effect, resulting in a curve exhibiting a minimum at moderate flowrate. Figure 12, a plot of percentage oil recovered outside of the cell versus carbon dioxide flowrate, demonstrates just such behavior.

Table 4:

PERCENTAGE OIL RECOVERED vs. CO_2 FLOWRATE at 306.1 K

The data given in this Table is plotted in Figure 12

FLOW RATE ft^3/min	OIL RECOVERED %	RETENTION TIME [illegible]	RUN#
0.172 ± 0.006	45.9 ± 3.9	22	23
0.118 0.007	41.0 3.3	22	24
0.257 0.008	10.0 0.8	3.5	25
0.382 0.009	14.3 1.1	3.5	26
0.052 0.001	53.1 4.2	22	27
0.061 0.002	29.4 2.4	3.5	28
0.292 0.009	55.2 4.4	22	29
0.136 0.003	35.5 2.8	22	30
0.153 0.005	13.0 0.9	3.5	31
0.168 0.004	6.1 0.5	3.5	32

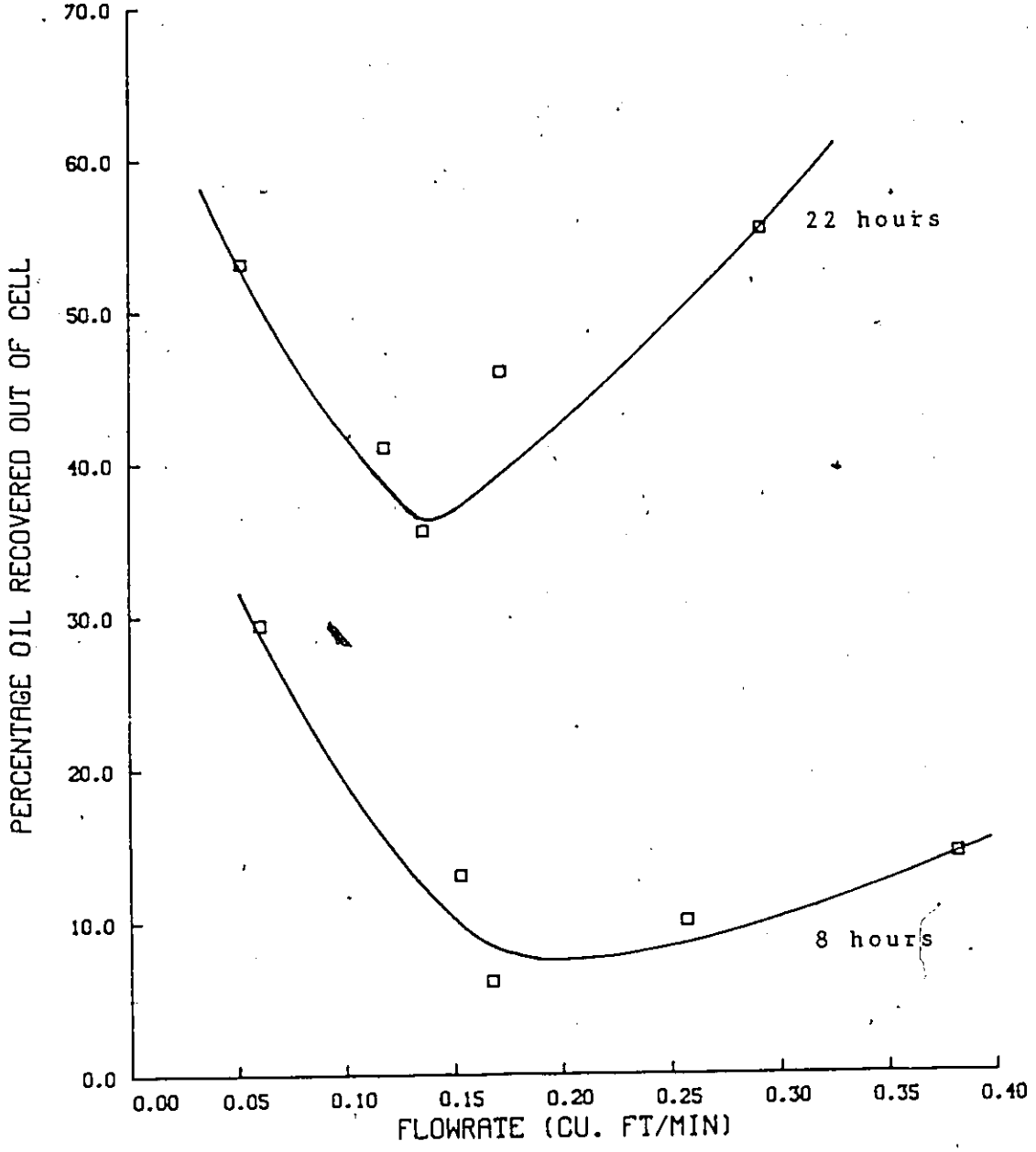

Figure 12: PERCENTAGE OIL RECOVERED vs. CO_2 FLOWRATE

The effect of retention time is clearly displayed by the difference in the two curves in Figure 11. As suggested by the reduced model, the retention time has a significant influence on the total oil removal from the chips. This would suggest that equilibrium within the cell has not been established at the lower retention time of 3.5 hours, nor at the static-stage lower boundary retention time of 8 hours. If we assume that equilibrium is established at the higher X4 value of 22 hours, then the range of possible values for the time required to reach equilibrium lies between 8 and 22 hours. Values obtained from the literature for the time required to reach equilibrium for comparable processes, using supercritical carbon dioxide as the solvent, fell in the range of 5 - 6 hours (8).

While the higher level of retention clearly leads to both improved oil removal and recovery, the advantages of a twenty-two hour retention time seem questionable, since roughly one-half the oil removal can be achieved with one-sixth the required retention. A two- or three-pass cycle with a 3.5 hour retention time could achieve roughly identical oil removal in under half the time of the twenty-two hour period. The ideal choice of retention time will of course be dictated by the more practical constraints of industry.

The effect of pressure on oil removal is plotted in

Table 5: OIL REMOVED vs. CO_2 PRESSURE at 306.1 K

The data given in this Table is plotted in Figure 13

PRESSURE p.s.i	OIL REMOVED g	RUN#
1118 ± 16	0.966 ± 0.013	32
1274 18	1.053 0.013	33
1416 22	1.251 0.024	34
1576 25	1.332 0.018	35
1724 25	1.331 0.019	36
2017 28	1.485 0.019	37
1883 27	1.423 0.018	38
2173 31	1.675 0.019	39

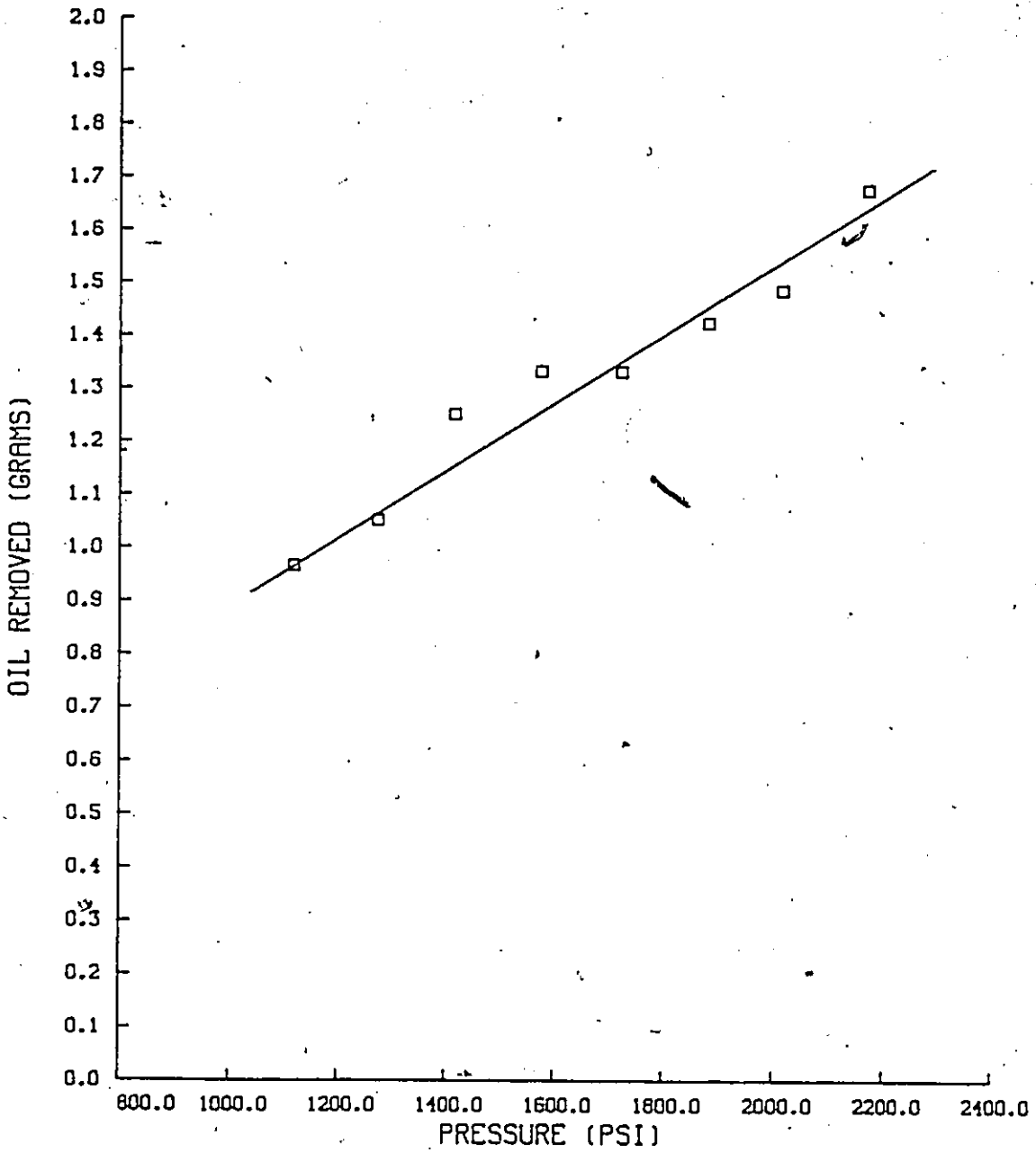

Figure 13: PLOT OF OIL REMOVED vs. CO_2 PRESSURE

Figure 13, from the data given in Table 5. As expected, this plot exhibited very nearly linear behavior with a strong positive slope over the range studied. During this stage of experimentation, the flowrate was kept constant at a value of 0.158 cubic feet per minute. Valve deterioration and replacement introduced a degree of variance in the actual flowrate (standard deviation = 0.023), but the choice of target flowrate was made in the region of the graph where vafiations in flowrate would produce the least effect on oil removal.

A plot of the oil recovery versus pressure is given in Figure 14 with complied data in Table 6; this plot as well serves to reveal the advantages of a high operating pressure. Over the range plotted (800 psi), the oil recovery increased by a factor of approximately four. Since the rate of increase can clearly not be expected to continue over 100%, we may assume that the upper portion of the curve (2100+ psi) approaches the maximum level of oil recovery.

Modelling the Data

The choice of the Chrastil equation as the fitted model lead to the very simple model form:

$$\ln d = k^{-1} (\ln c - a/T - b) \qquad (4.3)$$

Table 6:

PERCENTAGE OIL RECOVERED vs. CO_2 PRESSURE at 306.1 K

The data given in this Table is plotted in Figure 14

PRESSURE p.s.i	OIL RECOVERED %	RUN#
1274 ± 18	16.4 ± 1.3	33
1416 22	24.1 1.9	34
1576 25	28.6 2.3	35
1724 25	42.5 3.4	36
2017 28	52.4 4.2	37
2173 31	60.3 4.8	39

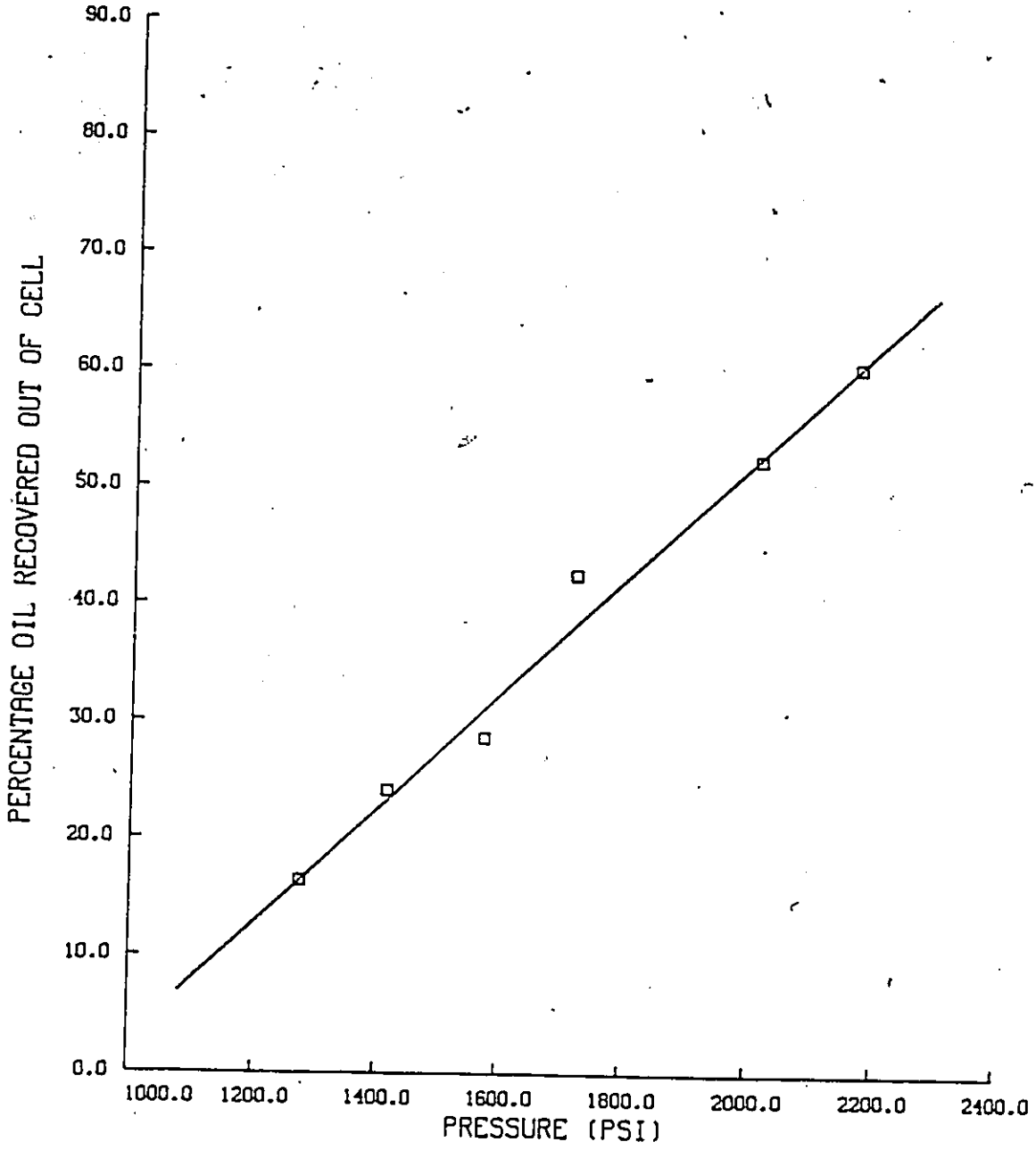

Figure 14: PLOT OF PERCENTAGE OIL RECOVERED OUT OF CELL vs. CO_2 PRESSURE

Data from Table 7 were fitted to this model. Since these data were obtained at a constant level of temperature, the terms involving temperature could be amalgamated into a single variable W:

$$\ln d = 1/k(\ln c) + W/k \qquad (4.4)$$

A simple linear fit of the data was sufficient to obtain the slope, 1/k, and the value of W. To obtain values for the parameters a and b, it was necessary to include runs from the factorial design which were conducted at the higher level of temperature, 38.0°C. The data used from stage one of the experiment were those runs for which T = 38.0°C and retention time was low (8 hours). The purge rate was ignored as having no influence on the response (as suggested by the least squares reduced model). Points were available for two levels of pressure, and the curve connecting these points was compared with the curve above to obtain a and b. Runs used from stage one of the data collection were #8, and #16 and #17 (replicates). The data and fitted response are presented in Table 7 and plotted in Figure 15. The final version of the model was:

$$\ln d = (1/0.501)(\ln c - (-41,300/T + 129.2)) \qquad (4.5)$$

Table 7:

CO_2 DENSITY vs. SOLUTE CONCENTRATION DATA at 306.1 K

The data given in this Table is plotted in Figure 15

DENSITY g/ml	SOLUTE CONCENTRATION g/ml (x 10^5)	RUN#
0.4744 ± 0.0135	90 ± 3	32
0.6896 0.0197	141 5	33
0.7319 0.0209	176 7	34
0.7622 0.0218	199 8	35
0.7834 0.0224	205 8	36
0.8151 0.0233	236 9	37
0.8019 0.0230	221 9	38
0.8283 0.0237	273 11	39

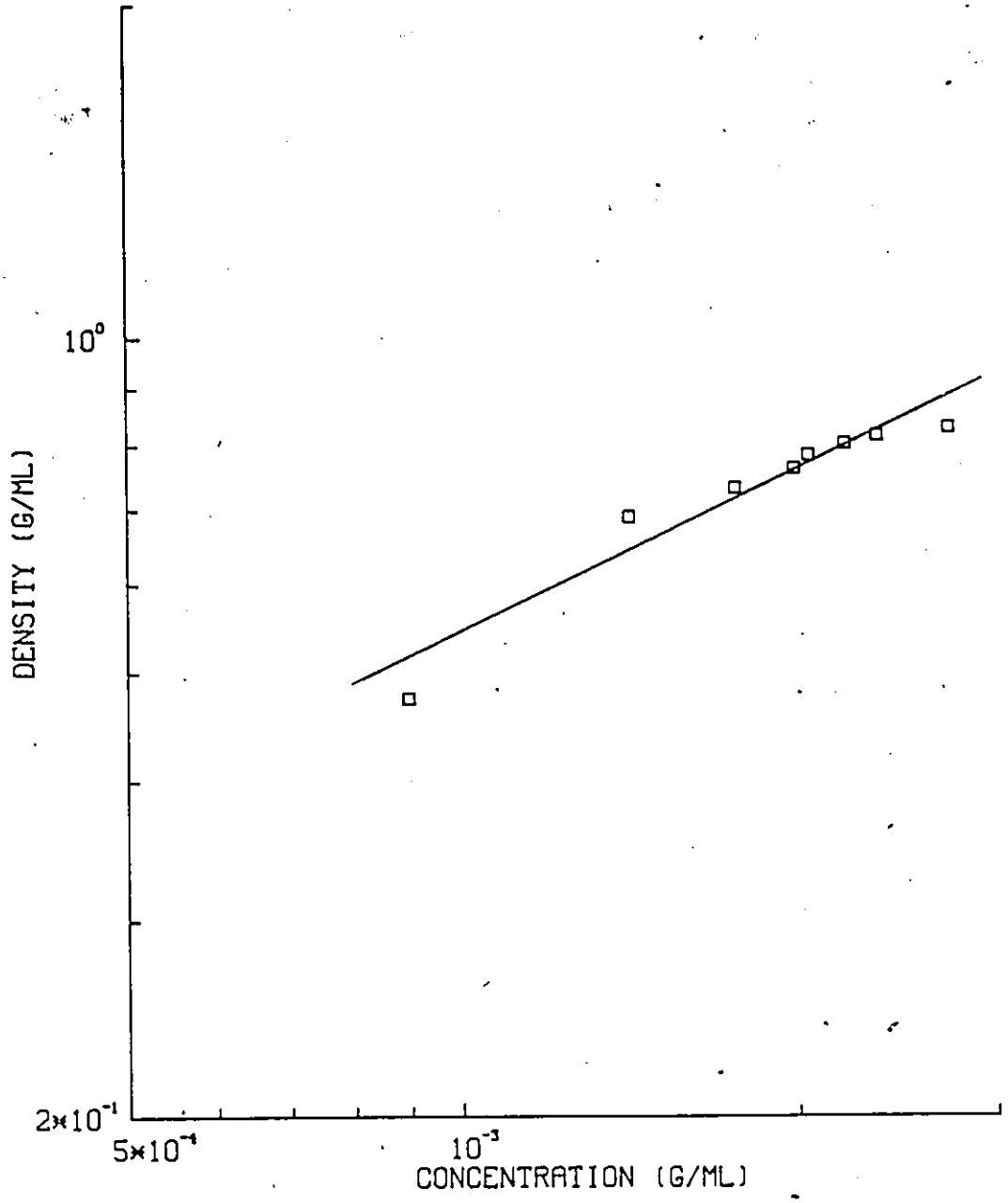

Figure 15: DENSITY OF CO_2 vs. CONCENTRATION OF SOLUTE

which yielded a sum of squares of residuals of 0.2326.

Qualitative Analysis of Product

In order to determine if the removal of a significant portion of the oil resulted in a noticeable difference in the taste of the chip, or if the process interfered with the product's flavour in any way, a double-blind taste test was conducted. Unlabelled samples of both untreated and treated chips with 22% oil removed were provided, and participants were instructed to chose the product they felt had the best taste. The test was conducted over two days and fourteen people were asked to repeat the test. The results (not including replicates) are tabulated below:

	TREATED	UNTREATED	NO PREFERENCE
DAY 1	12	12	7
DAY 2	9	4	5
	21	16	12

(SAMPLE SIZE = 49)

Of those with a preference, 57% chose the treated chips as having a better taste. To find if this quantity is statistically meaningful, a significance test was conducted on the data. For a test with greater than two possible

mutually exclusive outcomes, the probability of an outcome is calculated from a multinomial distribution:

$$P(X1,X2,X3) = \frac{N!}{X1!\ X2!\ X3!} (A_1)^{X1}(A_2)^{X2}(A_3)^{X3} \qquad (4.6)$$

where: N = NUMBER OF RUNS

Xi = NUMBER CHOOSING BRAND i

Ai = PROBABILITY OF SELECTING i

If we choose as the null hypothesis the supposition that there is no difference between the treated and untreated chips (i.e. $A_1=A_2=A_3$) then:

$$P(21,16,12) \text{ or better} = 9.1\% \qquad (4.7)$$

That is, it is more than 90% unlikely that a result this favourable would result from the test if we accept the fact that there is no difference in the taste of the chips.

Before this result can be accepted with confidence it is necessary that the reliability of the data be tested, i.e. it was required that the ability of the testers to actually determine a difference in taste be evaluated. The reliability of the data was determined by an analysis of the response of those who took the test on both days. Of the 14

people who repeated the test, only three made the same selection on both days. With this degree of variance in the data the results cannot be considered significant and we must accept the null hypothesis: that there is no noticeable difference in the taste and texture of the treated chips.

Chromatographic Analysis of Extracted Oil

While the product of the extraction process may be considered indistinguishable from the untreated product from a marketing standpoint, the question of potential changes in the nutritional value of the chip remains. While we may be confident that the bulk portion of the chip remains unchanged by the process, the composition of the oil remaining in the chip cannot be assumed identical to the original composition without testing. To compare the original oil composition with the extracted, a chromatographic analysis of each was performed. The chromatograph used was a Hewlet-Packard high pressure liquid chromatograph with a methyl column, model number 5830A. The solvent used was benzene.

Chromatographic plots of the original and extracted oil are given in Figures 16 and 17, respectively. An analysis of these plots reveals that the two samples are nearly identical; that is there is almost no difference in

composition between the vegetable oil in the chip and the oil which is extracted.

The results of the qualilitative analysis of the final product are reassuring, for they indicate with some confidence that there is no significant difference between untreated chips and those which have had as much as 22% of their oil removed. The results of the chromatographic analysis complete the requirements for a rounded analysis of the treated product.

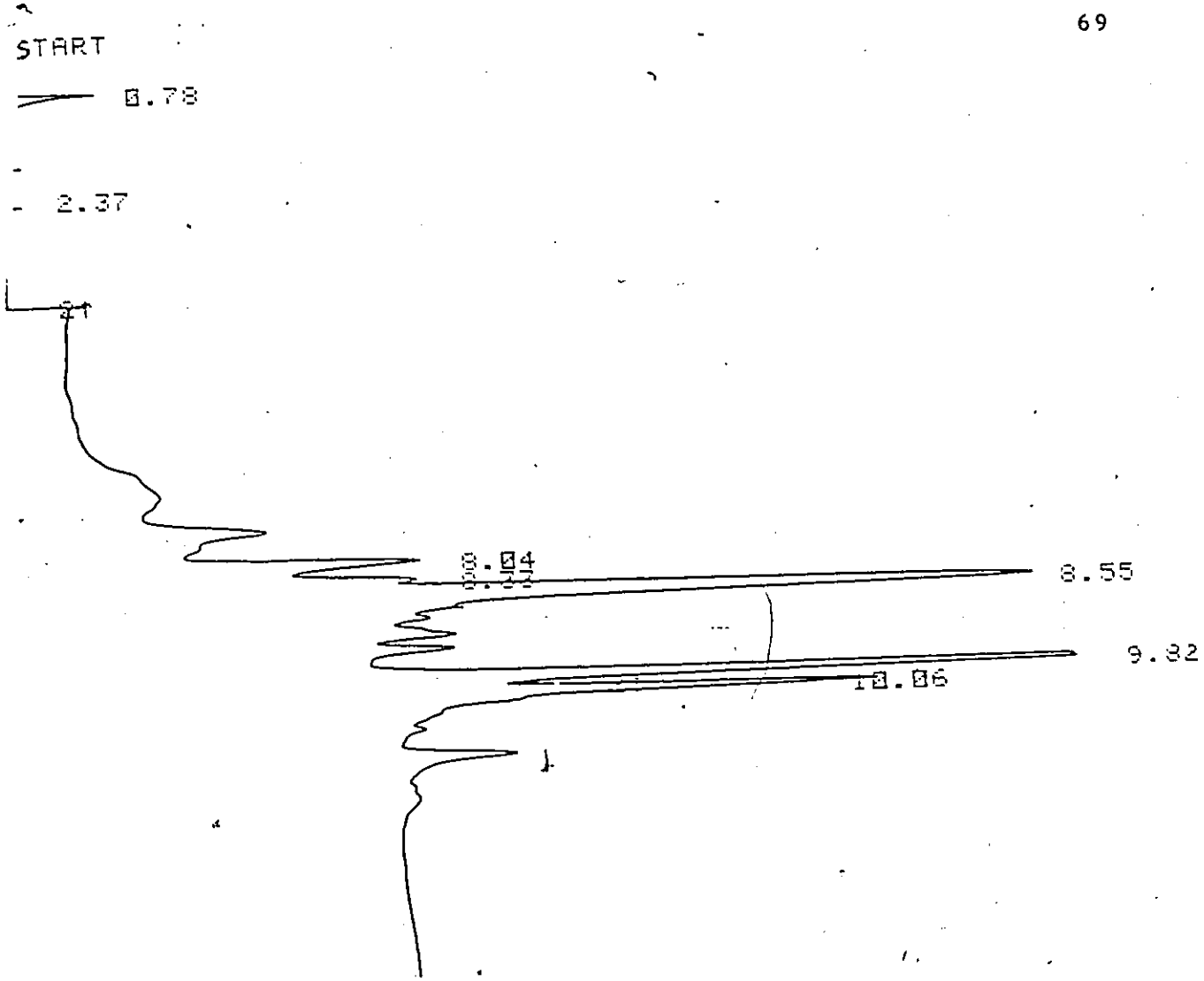

Figure 15: CHROMATOGRAPHIC ANALYSIS OF VEGETABLE OIL

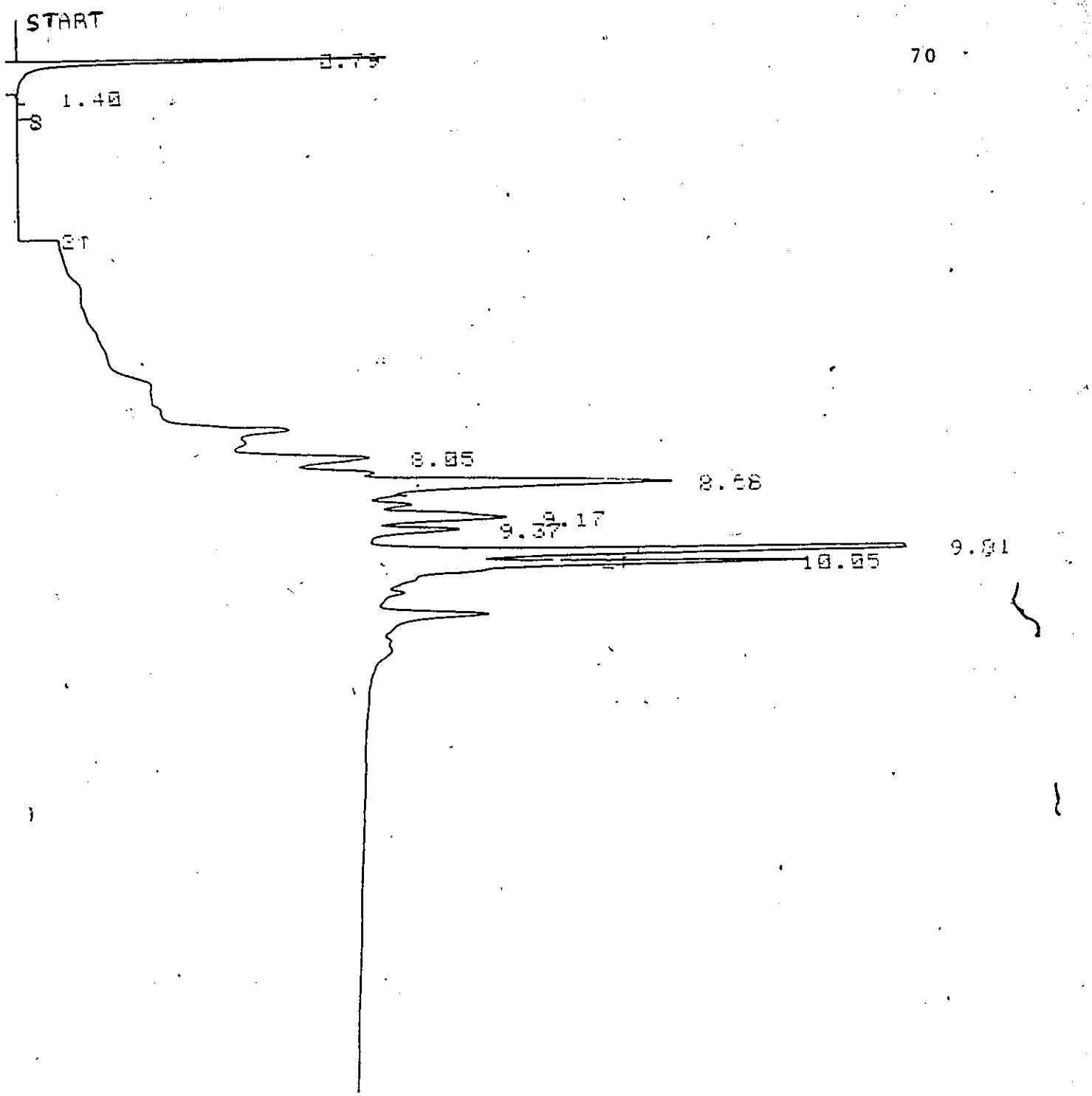

Figure 16: CHROMATOGRAPHIC ANALYSIS OF EXTRACTED OIL

Chapter V

CONCLUSIONS

In this work the practicality of the use of supercritical carbon dioxide to extract vegetable oils from potato chips has been examined. The success of such an extractive process is dependent upon the ability to produce a marketable product with a significant oil reduction, with capital and operating costs that are not prohibitive. This success hinges upon the location of the optimum operating region.

Of the two techniques studied, only the flow method offered the advantage of high oil recovery outside the cell. While the static method provided high oil removal, the problem of oil retention within the equilibrium cell proved detrimental. The flow method resulted in more consistent results and was chosen for the investigation of the pressure-solubility relationship. The elimination of the absorbent sponge within the equilibrium cell led to a higher oil recovery rate outside the cell.

The results of the first stage of investigation were useful in the design and implementation of the second stage of data collection. The period of time required to reach equilibrium within the cell is unexpected and not adequately explained. A method of mixing or otherwise agitating the

cell contents could lessen this period. The demonstrated dependency of solubility on temperature is in good agreement with the literature.

The fitted Chrastil equation provides a useful tool for estimating the solubility of vegetable oils in supercritical carbon dioxide, but should not be applied over a wide range of temperatures. A series of isotherms similar to Figure 13 over a suitable range of temperatures would prove useful for a more accurate estimation of the solubility parameters a and b.

The choice of optimum flowrate is simplified through the use of Figures 11 and 12, but care must be taken to select a flowrate which permits a rapid oil removal. While total oil removal is maximized as flowrate is reduced, the time required to remove the oil is greatly increased as we decrease the flowrate. A moderate flowrate may prove a necessary choice for an industrial process.

An excellent survivability and marketability of the product chips can be claimed with some confidence as a result of the qualitative and chromatographic analyses. No physical compacting or deformation of any kind was noted as a result of the process. Sufficient oil removal to arrive at substantial calorie reduction in the final product can be achieved without loss in product appeal.

Major sources of error for the experiments include

fluctuations in atmospheric pressure over the duration of the flow experiments, and the result of physically handling of products prior to and during weighing. When necessary gloves were used, but this did not prevent oil loss to walls of the cell or absorption by sponges and the nylon jacket. The volatility of the oil at the experimental temperature was not high, but samples for weighing were exposed to the atmosphere for the minimum possible period.

In an overall analysis, the data collected during the three stages of experimentation indicate that the removal and recovery of vegetable oil from potato chips using supercritical carbon dioxide is a potentially viable process. As a late stage in the manufacturing process it offers the dual advantages of providing recyclable oil and a diet product. While the choice of optimum operating region, with respect to flowrate, pressure and temperature, will ultimately depend on an economic analysis, the regions suggested by this work would appear to show the most promise.

Chapter VI

FURTHER RECOMMENDATIONS

The work conducted in characterizing the optimum operating region for the process has been far from comprehensive. The task of process optimization is complex and vast, and remains incomplete until on-line production testing is accomplished. The recommendations below are suggestions for future research based on the experimental work.

1) A quantitative analysis of the effect of temperature on solubility. The least squares fitted model suggests that substantial increases in oil solubility could be achieved through relatively inexpensive manipulation of process temperature.

2) An analysis of the time required for the system to attain equilibrium, and the effects of agitation and/or mixing.

3) The effect of solvent entrainers on the oil solubility. Recent work with such co-solvents

(entrainers) as water has demonstrated enhanced solubilities in the supercritical state for certain solutes; the possibility of increased oil solubility with such an entrained solvent is worthy of investigation.

REFERENCES

1) Hannay, J.B., Hogarth, J., Proc. Roy. Soc. (London), 29 , 324 (1879).

2) Kohn, P. and Savage, P., Chem. Eng., 86, 41 (1979).

3) Hubert, P. and Vitzthum, O., Ang. Chemie Int. Ed., 17 , 710 (1978).

4) Johnston, K.P., M.Sc. Thesis (unpublished), Dept. of Chem. Eng., University of Illinois, Urbana, Illinois (1979).

5) Schneider, G., Ang. Chemie Int. Ed., 17 , 716 (1978).

6) Worthy, W., C&EN, 80 , 16 (1981).

7) Superpressure Inc., Chem. Eng., 89 , 53 (1982).

8) Zosel, K., Ang. Chemie Int. Ed., 17 , 702 (1978).

9) Denis, M., Hostess Food Products, personal communication (1986).

10) Kirk, R.E. and Othmer, D.F., Encyclopedia of Chemical Technology , Vol. 6, Interscience Publishers Inc., New York (1951).

11) Margerum, M., M.Sc. Thesis, Dept. of Chem. Eng., University of Ottawa (1985).

12) Fillippi, R.P., Chem. Ind., 390 (June 1982).

13) Prausnitz, J.M., Molecular Thermodynamics of Fluid Phase Equilibria , Chap. 5, Prentice-Hall, Englewood Cliffs, N.J. (1969).

14) Redlich, O., and Kwong, J.N.S., Chem. Rev., 44 , 233 (1949).

15) Prausnitz, J.M., Lichtenhaler, R.N., and de Azevedo, E. G., Molecular Thermodynamics of Fluid Phase Equilibria, Second Edition, Prentice-Hall, Englewood Cliffs, N.J. (1986).

16) Chueh, R.L., Prausnitz, J.M., IEC Fundam., 6 , 492 (1967).

17) Robin, S. and Vodar, B., Faraday Soc., 36 , 233 (1953).

18) Stahl, E., Schilz, W., Schultz, E., and Willing, E., Angew. Chem. Int. Ed., 17 , 731-738 (1978).

19) Chrastil, J., J. Phys. Chem., 86 , 3016 (1982).

20) Adachi, Y., Lu, B.C.-Y, Fluid Phase Equ., 14 , 147 (1983).

21) Angus, S., Armstrong, B., and deReuck, K.M., International Thermodynamic Tables of the Fluid State, Carbon Dioxide, Pergamon Press, Oxford (1976).

22) Basta, Nicholas, Chem. Eng., 92 , 14 (1985).

23) Sims, M., Chem. Eng., 89 , 50 (1982).

24) O'Toole, C., Richmond, P., and Reynolds, J., Chem. Eng., 425 ,73 (1986).

APPENDIX A

RAW DATA

The solubility measurements made in this work are given in this appendix. The data are organized into three separate tables. Table A lists data for the eleven runs used in the factorial design; Table B gives raw data for the ten constant pressure runs used in Figures 11 and 12; and Table C lists the eight constant temperature runs used in the compilation of Figures 13 to 15. Data are given in the units in which they were originally recorded. Oil recovery is given in terms of oil recovered outside the cell only for Tables B and C.

Table A: RAW DATA FOR RUNS 1 - 11

TEMP °C	PRES psi	ATMOS. PRES mm Hg	PURGE RATE min	RETEN. TIME hrs	TOTAL CO_2 ft^3	OIL REMOVED g	OIL RECOVERED g	RUN#
33.0	1122	757.2	11.42	24	3.98	2.692	2.243	1
38.1	1119	756.8	0.76	24	3.89	3.465	2.683	2
33.1	1070	753.9	10.33	8	3.92	1.565	1.553	3
38.1	1072	758.4	10.07	24	3.43	3.327	2.593	4
38.0	1072	747.4	0.83	8	3.80	1.564	1.410	5
33.0	1120	766.4	10.04	24	3.86	1.923	1.757	6
33.0	1120	760.3	1.07	8	3.60	1.395	1.390	7
33.0	1073	758.7	0.92	24	3.38	2.912	1.910	8
33.0	1071	757.9	8.18	8	2.91	1.806	1.863	9
38.0	1122	753.7	8.25	8	2.92	1.578	1.701	10
38.0	1120	758.8	10.48	8	2.48	1.850	1.749	11

Table B: RAW DATA FOR RUNS 23 - 32

TEMP °C	PRES psi	ATMOS. PRES mm Hg	FLOW RATE ft^3/min	RETEN. TIME hrs	TOTAL CO_2 ft^3	OIL REMOVED g	OIL RECOVERED g	RUN#
33.1	1120	767.1	0.172	22	10.29	1.947	0.760	23
33.0	1139	759.0	0.118	22	10.29	1.953	0.626	24
33.0	1130	754.6	0.257	3.5	10.26	0.958	0.100	25
33.1	1127	757.8	0.382	3.5	10.31	0.953	0.146	26
33.1	1120	760.8	0.052	22	10.25	2.663	1.030	27
33.0	1120	767.6	0.061	3.5	10.31	1.206	0.313	28
33.0	1122	751.0	0.292	22	10.23	2.236	1.030	29
33.0	1119	762.7	0.136	22	10.24	1.753	0.465	30
33.0	1120	752.2	0.153	3.5	10.28	0.813	0.104	31
33.0	1118	763.6	0.168	3.5	10.23	0.966	0.057	32

Table C: RAW DATA FOR RUNS 33 - 39

TEMP °C	PRES psi	ATMOS. PRES mm Hg	FLOW RATE ft^3/min	RETEN. TIME hrs	TOTAL CO_2 ft^3	OIL REMOVED g	OIL RECOVERED g	RUN#
33.1	1274	764.8	0.123	3.5	10.24	1.053	0.165	33
33.0	1416	764.2	0.135	3.5	10.37	1.251	0.285	34
33.0	1576	755.7	0.180	3.5	10.23	1.332	0.348	35
33.0	1724	755.8	0.146	3.5	10.23	1.331	0.557	36
33.0	2017	759.3	0.197	3.5	10.25	1.485	0.773	37
33.0	1883	765.6	0.174	3.5	10.24	1.423	0.703	38
33.0	2173	753.2	0.158	3.5	10.26	1.675	1.006	39

APPENDIX B

EQUATION OF STATE FOR CARBON DIOXIDE AND COMPUTER PROGRAM

A high precision equation of state has been developed to accurately predict the compressibility factor, and thus the density, of carbon dioxide over a wide range of temperatures by IUPAC (21). This appendix gives this equation and the listing of a computer program written for its use.

The IUPAC equation for carbon dioxide is

$$Z = 1 + \sum \sum b_{ij} (1/T_r - 1)^j (\rho_r - 1)^i \qquad (B.1)$$

where ρ_r is the reduced density and T_r is the reduced temperature. The critical density and temperature of carbon dioxide are 0.01063 mol/cm and 304.2 K, respectively. The values for the coefficients b_{ij} are given in the computer program.

```
C
C     THIS PROGRAM CALCULATES THE COMPRESSIBILITY FACTOR
C     OF CARBON DIOXIDE USING THE THE ANALYTIC EQUATION OF
C     STATE DEVELOPED BY IUPAC
C
C     VARIABLES USED:
C
C               T = TEMPERATURE (K)
C               P = PRESSURE (MPA)
C              RO = DENSITY OF CO2 (GMOL/ML)
C          B(I,J) = PARAMETERS OF THE EQUATION OF STATE
C               Z = COMPRESSIBILITY FACTOR
C       Z1,Z2,Z3 = VALUES OF Z USED IN THE CONVERGENCE
C                  ROUTINE
C          F1,F2 = VALUES OF THE CONVERGENCE FUNCTION
C
C
C    REFERENCE:
C          ANGUS, S., ARMSTRON, B. AND K.M. DEREUCK
C          INTERNATIONAL THERMODYNAMIC TABLES OF THE FLUID STATE, CO2
C          PERGAMON PRESS, OXFORD (1976)
C
C    PROGRAM HISTORY
C
C          (1985) PROGRAMMED BY M. MARGERUM
C          (1987) MODIFIED BY J. O'NEILL
C
      DIMENSION B(10,7)
      DO 100, I = 1,10
         DO 200 J = 1,7
         READ(5,*) B(I,J)
200      CONTINUE
100   CONTINUE
      T = 306.1
      P = 7.717
      Z1 = 0.258
      Z2 = 0.0
      CHECK = (0.000005)**2
      Z = Z1
      CALL MIKE(Z,B,T,P)
      F1 = Z1-Z
      DO 300 K = 1,200
         Z = Z2
         CALL MIKE(Z,B,T,P)
         F2 = Z2-Z
         Z3 = (Z2*F1 - Z1*F2)/(F1-F2)
         Z1 = Z2
         Z2 = Z3
         F1 = F2
         ZIPPO = F2**2
         IF(ZIPPO.LT.CHECK) GOTO 2
300   CONTINUE
2     ABC=((Z2*100000)+0.5)/100000
      WRITE(6,3) ABC
3     FORMAT(/,'CO2 COMPRESSIBILITY FACTOR =',F10.9)
```

```
      STOP
      END
C
C
      SUBROUTINE MIKE(Z,B,T,P)
      DIMENSION B(10,7)
      RO = P/(Z*T*8.314)
      WRITE(6,99) RO
   99 FORMAT('THE CO2 DENSITY IS: ',F10.8)
      Z = 0.
      DO 11 I = 1,10
         DO 22 J = 1,7
            Z = Z +B(I,J)*(304.2/T -1)** (J-1)*(RO/.01063 -1)**(I-1)
C           WRITE(6,*) B(I,J)
   22    CONTINUE
   11 CONTINUE
      Z = 1 + Z*RO/.01063
      WRITE(6,9) Z
    9 FORMAT('THE VALUE OF Z IS: ',F10.8)
      RETURN
      END
```

```
-.723354437
-.168332974E1
 .259587221
 .376945574
-.67075537
-.871456126
-.149156928
 .447869183
 .126050691E1
 .596957049E1
 .154645885E2
 .194449475E2
 .864880497E1
0.0
-.172011999
-.183458178E1
-.461487677E1
-.382121926E1
 .360171349E1
 .492265552E1
0.0
 .446304911E-2
-.176300541E1
-.111436705E2
-.278215446E2
-.271685720E2
-.642177872E1
0.0
 .255491571
 .237414246E1
 .750925141E1
 .661133318E1
-.242663210E1
-.257944032E1
0.0
 .594667298E-1
 .116974683E1
 .743706410E1
 .150646731E2
 .957496845E1
0.0
0.0
-.147960010
-.169233071E1
-.468219937E1
-.313517448E1
0.0
0.0
0.0
 .136710441E-1
-.100492330
-.163653806E1
-.187082983E1
0.0
0.0

0.0
 .392284575E-1
 .441503812
 .886741970
0.0
0.0
0.0
0.0
-.119372097E-1
-.846051949E-1
 .464564370E-1
0.0
0.0
0.0
0.0
```

APPENDIX C

CONFIDENCE INTERVALS FOR THE FITTED PARAMETERS

Using the replicates provided by the factorial design we may determine a 95% confidence interval for each of the fitted parameters in the response function (see page 49). Those parameters for which such an interval includes the value zero may be dropped from the equation, resulting in a reduced model.

The replicates provided by the factorial design are

$$\text{RUNS \# 3\&9:} \quad Y = 1.5647,\ 1.8060 \quad (Y_1 = 1.6854) \qquad \text{(C.1)}$$

$$\text{RUNS \# 10\&11:} \quad Y = 1.5770,\ 1.8504 \quad (Y_2 = 1.7140) \qquad \text{(C.2)}$$

$$\text{RUNS \# 1\&6:} \quad Y = 1.9229,\ 2.6922 \quad (Y_3 = 2.3076) \qquad \text{(C.3)}$$

If we assume the variance does not change over the range of the experiment, we may estimate the sample variance s^2 as

$$s^2 = \frac{1}{n-1} \sum_{i=1}^{n} (Y_i - Y)^2 \qquad \text{(C.4)}$$

$$= 0.0604$$

This estimate has n-1 = 5 degrees of freedom. We may arrive at a 95% confidence interval for the $\hat{B}$'s (parameters) with the use of the t-table and the following equation:

$$\hat{B} \pm t_{5,.02}(.0604/11)^{1/2} \qquad (C.5)$$
$$= \hat{B} \pm 2.571(.0741)$$
$$= \hat{B} \pm 0.190$$

APPENDIX D

CALIBRATION CURVE FOR PRESSURE TRANSDUCER

This appendix contains the calibration curve for the Sonotek SA pressure transducer, serial number 13429. The transducer was calibrated on October 4, 1985, using precision weights.

Two curves are provided in the calibration plot (Figure A); one is used while reading down, i.e. as the pressure decreases, and the other is used while reading up, or as the pressure is increasing. The corrective terms provided by these plots are added to the transducer reading to give the actual pressure.

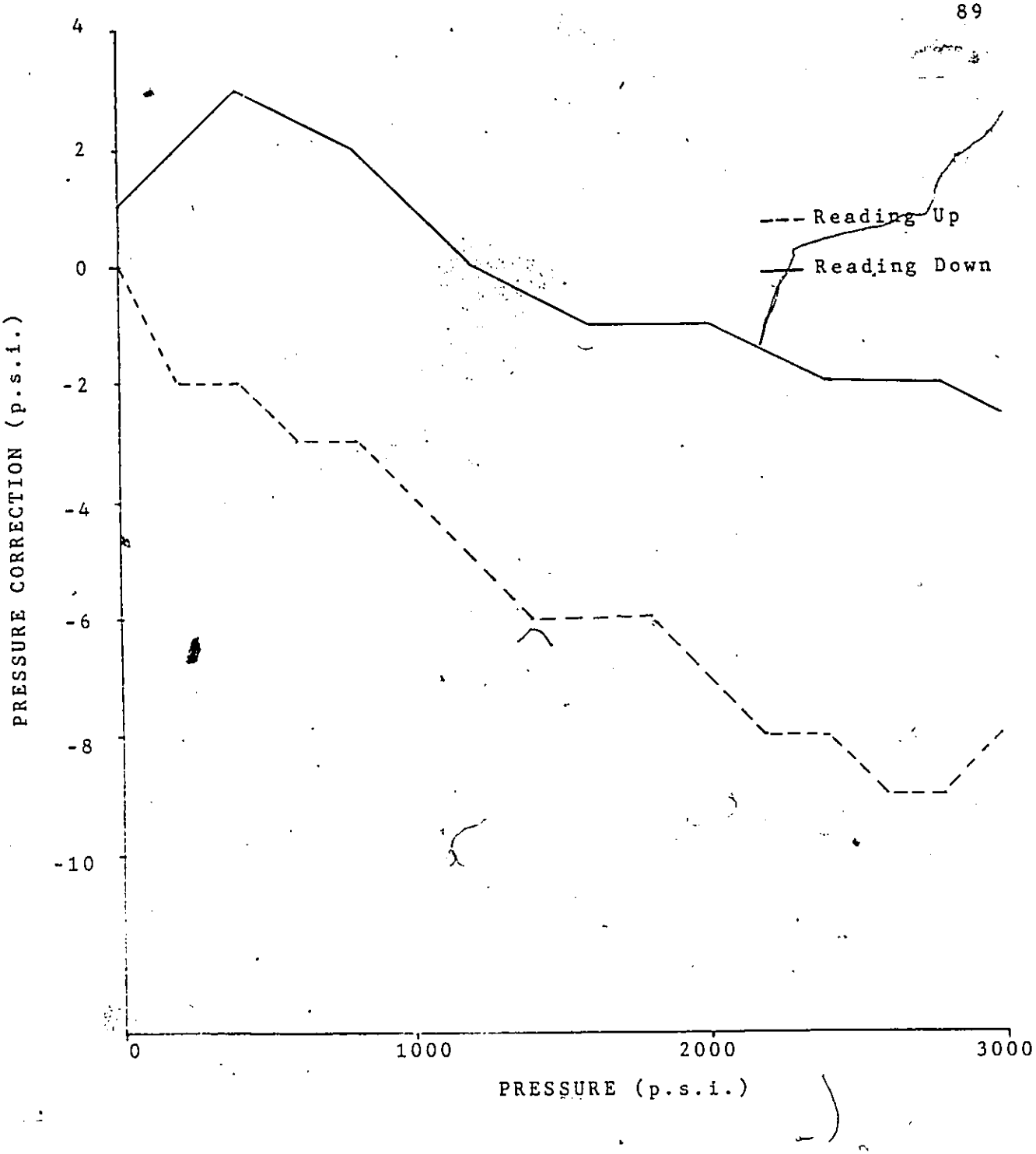

Figure A: CALIBRATION CURVE FOR PRESSURE TRANSDUCER